Control of Autonomous Underwater Vehicles

Raja Rout

Department of Electrical Engineering
National Institute of Technology,Rourkela
Rourkela-769008, Odisha, India
Jan 2013

Control of Autonomous Underwater Vehicles

A thesis submitted in partial fulfillment of the
requirements for the award of the degree of

Master of Technology by Research

in

Electrical Engineering

by

Raja Rout
Roll-609EE103

Under the Guidance of

Prof. Bidyadhar Subudhi

and

Prof. Sandip Ghosh

Department of Electrical Engineering
National Institute of Technology Rourkela
2010-2012

Department of Electrical Engineering

National Institute of Technology, Rourkela

C E R T I F I C A T E

This is to certify that the thesis entitled ***"Control of Autonomous Underwater Vehicles"*** *by* ***Mr. Raja Rout****, submitted to the National Institute of Technology, Rourkela (Deemed University) for the award of Master of Technology by Research in Electrical Engineering, is a record of bonafide research work carried out by him in the Department of Electrical Engineering , under my supervision. We believe that this thesis fulfills part of the requirements for the award of degree of Master of Technology by Research.The results embodied in the thesis have not been submitted for the award of any other degree elsewhere.*

Prof. Bidyadhar Subudhi ***Prof. Sandip Ghosh***

Place:Rourkela
Date:

To My Loving parents, brother, sister-in-law, sister, brother-in-law and Ridhiman

Acknowledgements

First and foremost, I am truly indebted to my supervisors Prof. Bidyadhar Subudhi and Prof. Sandip Ghosh for their inspiration, excellent guidance and unwavering confidence through my study, without which this thesis would not be in its present form. I also thank them for their gracious encouragement throughout the work.

I express my gratitude to the members of Masters Scrutiny Committee, Professors D. Patra, S. Samanta, D. R. K. Parhi and K. C. Pati, for their advise and care. I am also very much obliged to Head of the Department of Electrical Engineering, NIT Rourkela for providing all the possible facilities towards this work. Thanks also to other faculty members in the department.

I would like to thank Basant, Dushmanta, Srinibas, Rakesh, Abhishek, Satyam, Santanu, Koena and other research scholars at Center for Industrial Electronics and Robotics(CIER), NIT Rourkela, for their enjoyable and helpful company.

My wholehearted gratitude to my beloved parents, Promodini and Ashok Ku. Rout for their encouragement and support.

Abstract

Autonomous Underwater Vehicles find extensive applications in defense organizations for underwater mine detection and region surveillance. These are also useful for oil and gas industries in detection of leakage in the pipelines and also in many other marine industries. Underwater Robots can be categorized into two types namely (i) Remotely Operated Vehicle (ROV) and (ii) Autonomous Underwater Vehicle (AUV). A ROV is a remotely operated vehicle usually connected with the mother ship or base station through a tethered wire whereas AUV is an Autonomous Underwater Vehicle which traverses autonomously without any external interference. As opposed to ROV, control of an AUV is difficult because it is an underactuated system (whose actuator inputs are less than the number of degrees of freedom to be controlled), also the dynamics of AUV is influenced by external disturbances such as ocean current and hydrodynamic effects. The motion control problems of an AUV can be of different types such as path following, trajectory tracking, waypoint tracking and also localization.

The thesis first develops path following control of a single AUV using the Serret-Frenet(S-F) frame approach and error backstepping technique. Later on the same backstepping approach has been extended for implementation of formation control for multiple AUVs.

Out of various motion control strategies, this thesis mainly focusses on path following control problem of a single AUV. To address this problem of path following, a virtual frame is considered. This virtual moving frame is called the S-F frame. The purpose of using S-F frame is to represent the AUV kinematics in terms of virtual frame parameters. Then a suitable control strategy has been developed which generates appropriate thruster force and rudder orientation enabling the AUV to follow the desired path. In the thesis, the path following controller has been developed using the concept of error backstepping method. In the developed controller it is also shown that the path following error i.e. distance between virtual frame and AUV actual frame approaches to zero and it is also ensured that other states of the AUV remain stable and bounded. Although error backstepping approach has been employed for path following problem but the earlier work [1] has not

considered the surge motion dynamics and coupling of rudder angle. Therefore, this thesis has addressed the limitation of [1] and developed the backstepping controller considering the rudder coupling term.

Although using a single AUV has many advantages but in case of its failure, the complete mission may be affected. Further, the area coverage by an individual AUV is limited. Thus, multiple AUVs are deployed for achieving a co-operative operation. Co-operative working of multiple AUVs obviate the aforesaid disadvantages as the group of AUVs in co-operative motion provides robustness in case of an individual AUV failure. Recently, a lot of research has been directed on developing cooperative motion control of multiple AUVs. Co-operative motion control can be achieved through different control strategies such as Leader-Follower, Virtual Based structure and Behavior Based Formation Control. These cooperative control strategies have their own advantages and disadvantages. Hence, these strategies have been reviewed and in this work, the concept of S-F together with error backstepping approach have been exploited to develop formation control of multiple AUVs. A fuzzy logic controller has also been implemented for deriving the control algorithm for leader-follower formation control scheme applied to control a group of AUVs.

Subsequently, the thesis presents a graphical simulation environment using VRML and SIMULINK3D to visualize the effect of controllers developed in providing the desired path following and formation control activities of AUV(s). This graphical simulation accepts the AUV states as inputs and represents the motion in an oceanic environment.

Also a proposal on hardware set up design of a single AUV is presented in the thesis. The selection of necessary sensors, actuators and various electronics components for the AUV hardware have been presented.

Contents

List of Abbreviations

Abbreviation	Description
AUV	Autonomous Underwater Vehicle
DoF	Degree of Freedom
DVL	Doppler Velocity Log
UAV	Unmanned Aerial Vehicle
S-F	Serret-Frenet
INS	Inertial Navigation System
GPS	Geostationary position System
USBL	Ultra Short Baseline
FFI	Forsvarets Forsknings Institute
NIO	National Institute of Oceanography
VRML	Virtual Reality Modeling Language
CSIR	Council of Scientific and Industrial Research
CMERI	Central Mechanical Engineering Research Institute
FLC	Fuzzy Logic Controller
IMU	Inertial Measurement Unit
NACA	National Advisory Committee for Aeronautics
ROV	Remotely Operated Vehicle
SBC	Single Board Computer
LOM	Largest of Maxima
MOM	Middle of Maxima
SOM	Smallest of Maxima
PWM	Pulse Width Modulation
DSP	Digital Signal Processing

List of Figures

List of Tables

Chapter 1

Introduction

1.1 Autonomous Underwater Vehicle(AUV)

AUV refers to an autonomous robot equipped with suitable sensors and actuators which enable it to navigate in the subsea environment. This is an autonomous robot because it executes the assigned mission without any external human intervention.

1.2 Background

Since the last decade, the control of AUVs has attracted attention of many researchers around the world. Control of AUV with autonomy refers to the ability of AUV to navigate in underwater environment without any human intervention. The autonomous navigation and control of an AUV in oceanic environment is a challenging task due to the fact that the dynamics of AUV is very complex, time varying, nonlinear and uncertain.

AUVs find application in oil industries, defense and research organizations. Some of these are as follows.

- AUV find applications for sea floor mapping or hydrographical surveys for the development of subsea infrastructure or layout of pipelines for oil/gas industries [4, 5]. AUVs are also employed for the leakage detection of oil/gas from the underwater pipelines. The usage of AUV offers great benefits in replacing human operator thus avoiding the operating cost and risk in the extreme environment i.e. deep oceanic environment. Some of the AUVs which are generally used for commercial purpose are shown in Fig1.1a. It has been developed by Kongsberg Maritime and Forsvarets Forsknings Institute (FFI) in Norway,Bluefin AUV by Bluefin Robotics.
- AUVs are also suitable for military applications and for underwater mine detection. AUVs can also be used anti-submarine warfare and also employed in a protected area for identification of unauthorized trespassing. In recent years, AUVs are being used

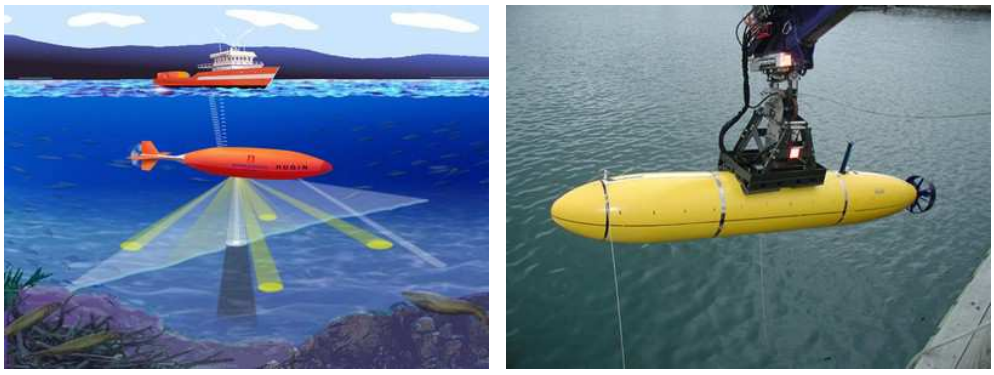

(a) HUGIN AUV [6] (b) Bluefin 12s AUV [7]

Figure 1.1: Examples of Commercial AUV's

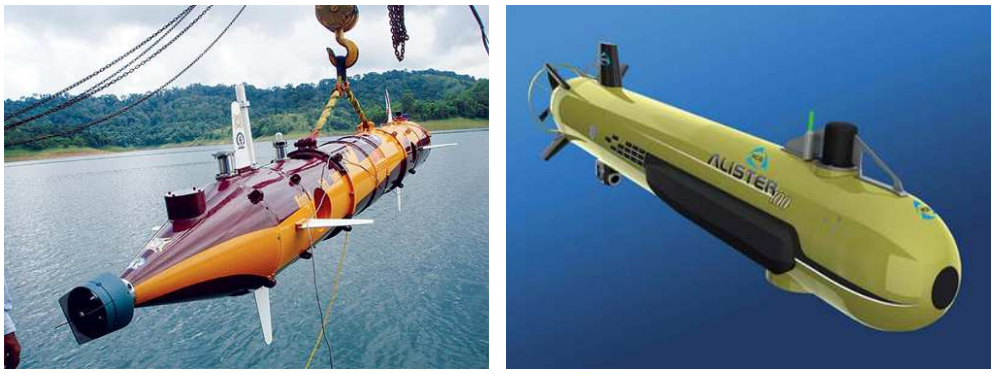

(a) AUV150 [8] (b) ALISTER100 [9]

Figure 1.2: Examples of Military application AUV's

as means for providing warfare equipments and medicines to the affected area. Few AUVs which are known for their application in defense and other military application are AUV150 by CSIR-CMERI, India, TALISMAN by BAE Systems and ALISTER 100 by eca Robotics.

- AUVs play a major role for marine industries because AUVs have ability of collecting data with minimal disturbance and with great accuracy. An AUV can also be used for study of water quality at reservoirs/dams and also for checking the dissolved oxygen level required for sustaining marine life. Some of the AUVs used for marine research or environmental studies are MAYA AUV by NIO, India, MARUM AUV by University of Bremen and SeaCat AUV by RUVSA.

In order to employ an AUV for a particular application, it is required that it should be equipped with appropriate sensors to acquire the signals of interest for monitoring and control. For navigation of an AUV, a fusion of sensors such as Inertial Navigational System(INS),Geostationary Position System(GPS) are sufficient for getting the exact position and orientation. But the problem with GPS is that it does not work in underwater

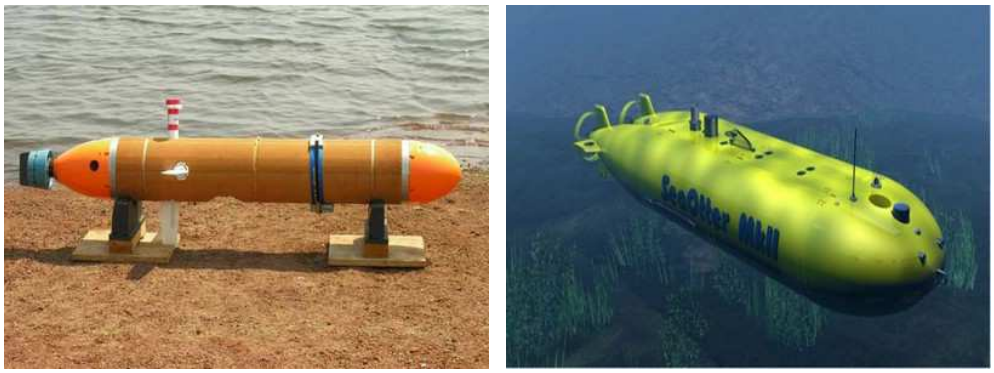

(a) MAYA AUV [10, 8] (b) SeaCat AUV [11]

Figure 1.3: AUV's used for oceanography and marine studies

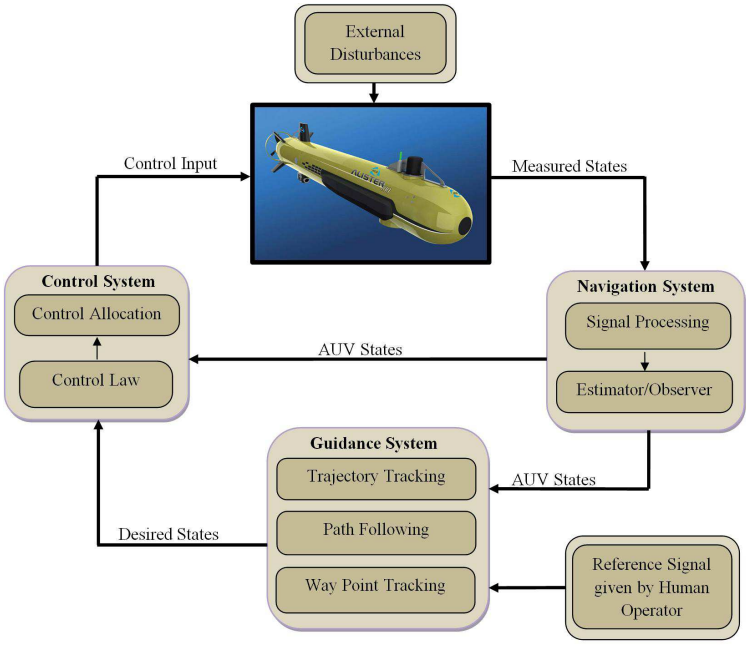

Figure 1.4: Structure of an AUV showing Navigation,Guidance and control schemes

environment, So in this case, a Doppler Velocity Log(DVL) can be employed i.e. a sensor fusion of INS/GPS/DVL is necessary. From DVL sensor, one can get accurate velocity reading because it calculates the velocity parameter from the rate of change of seabed. These are the primary sensors for navigation purpose, whereas sonar and camera can be used for object detection and obstacle avoidance. There is a need of specific sensors which are used for particular application.

1.3 AUV Structure

Most of the applications of AUV require that it should follow a desired path like pipeline or scanning or surveillance of a desired region, these requirements lead to address a common

objective for most of the applications is navigation.

1.3.1 Navigation System

Navigation system is meant for obtaining the position and orientation of the vehicle using INS, GPS, or other acoustic sensors. But the navigation of an AUV is difficult because the unavailability of the sensors for giving accurate position and orientation measurements. But with the development of DVL, Ultra Short Baseline(USBL) and many other position measurement sensors, which can be integrated to the INS for getting accurate data. In the navigation system, usually the sensor data get corrupted by external noises. So signal processing has a major role in navigation system. If a state is unavailable then an estimator can be employed to generate the missing or unmeasured state.

1.3.2 Guidance System

The guidance system deals with the desired path generation from AUVs current position to the desired position. The major challenge in the guidance control is to generate an optimum path for the AUV considering the obstacles between the paths. It is also necessary for the AUV to follow the optimum path successfully, for this, the path feasibility for the particular AUV should be determined. The feasible path will differ for different AUVs depending on whether it is a fully-actuated or an underactuated system.

1.3.3 Control Structure

Control structure determines the required control forces necessary for steering the AUV along the desired path, different objectives which can be addressed by the control structure are trajectory tracking, path following and way point tracking. While developing a control law, it is necessary to check the stability of the AUV states, and also the generated control forces should reside within its maximum limit. Design of control law for a fully-actuated system is simpler than an underactuated system but the control allocation map is to be given major attention. In an underactuated system, it is challenging to develop a control law together with ensuring the system stability. For both the cases it is necessary to show the robustness and adaptation of the control structure for the external disturbances.

This focus of this thesis is to develop control algorithms for an AUV to accomplish path following of a desired path. Besides path following, other motion control strategies of interest are trajectory tracking and way point tracking, which are described as follows.

- Trajectory Tracking Problem: It refers to the control problem where the AUV is required to follow a time-parameterized path. But the degree of complexity for controller development is highly dependent on whether the system is fully-actuated or under-actuated. It is not always reasonable to use a fully-actuated system because

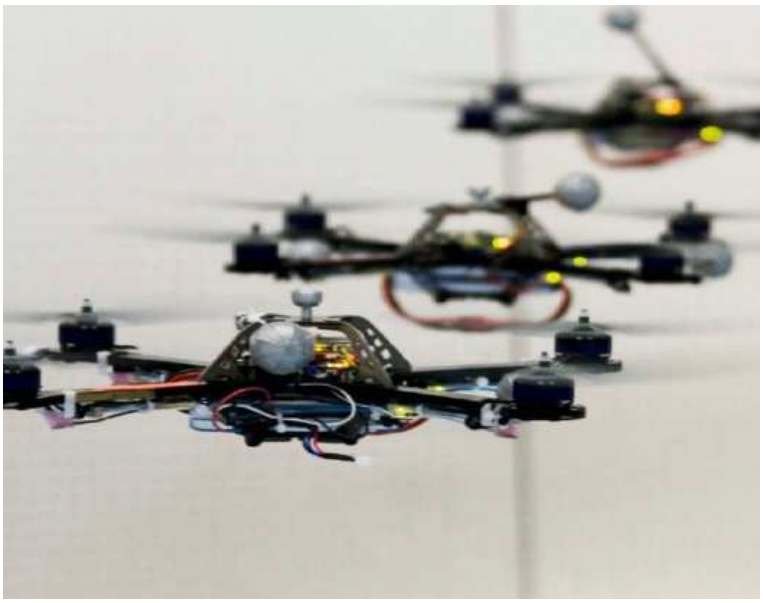

Figure 1.5: Formation of Quadrotor [*courtesy* : *FRAC*]

of its cost, weight and efficiency consideration. Trajectory tracking problem can be well defined for fully-actuated system. But it is still an active area of research for underactuated system.

- Path Following Problem: Unlike the time parameterized point as desired for trajectory tracking problem, here an entire path is considered for tracking without any time-parameterized constraint. Path-following is well suited for underactuated system because less number of constraints involved. For path-following problem the path is represented with its geometrical description and the AUV needs to follow the geometrical property of the path and eventually converges to the path .

- Way Point Tracking Problem: Unlike the trajectory tracking and path following problems, way point tracking problem is different. Here, an AUV does not follow a path rather a desired region is specified within a visible range. The control force should be such that it will drive the AUV towards the region confirming the stability criteria. In this approach, a series of way-points are placed between the AUV actual position and desired position. The objective of this problem is control AUV so that it reaches the desired position following the way-points. For this reason, this approach is called way-point tracking.

1.4 Cooperative Motion

Though there are numerous advantages of using a single AUV as discussed in Section 1.2 but there are some limitations in using a single AUV. With the addition of sensors for

achieving accurate measurement of position and orientation, the cost of an AUV increases also the payload of the AUV increases. The vehicle failure can affect the complete mission and also if numerous data are to be collected then the operating cost for an AUV increases. These limitations can be overcome by using multiple AUVs because for single AUV failure other AUVs in the group can still work and also the data collection by multiple AUVs will be faster and secured. The technological advancement in AUV research has raised the interest among the researchers for cooperative motion. Cooperative motion of AUVs refers to the motion of multiple AUVs for a common objective. To achieve the same, these AUVs communicate with each other. AUVs share the data received by each AUV and takes a common decision considering the feasibility and constraints. Due to these features, the cooperation among the AUVs can address the problem of single AUV failure and robustness for unknown terrain. Fig.1.5 shows the cooperative control of quadrotors. Some of the other robots/systems employed in formations are described as follows.

- Mobile Robot: Cooperative control of a group of mobile robots is adopted in many tasks such as in task allocation, object transportation and sensor network etc. For cooperative control, multiple robots [12, 13] should maintain a geometrical pattern or form a group to follow a desired path or trajectory. Some of the outdoor applications of multiple mobile robots are security patrols, handling hazardous materials and reconnaissance in missions etc.

- Satellite Formation: Satellite Formation is an approach to combine group of smaller satellites to work together or replacing a larger and more expensive satellite. The advantages of using behind the formation of satellite [14] is that it reduces the build time, simpler designs and sensing capability is increased. The applications which can be accomplished by formation of satellites are interferometry, environmental and communication applications etc.

- Formation of UAV: Like mobile robots multiple UAVs also can be engaged for area coverage and reconnaissance. A formation of multiple UAVs [15, 16] can also be used for environmental analysis.

1.4.1 Formation Control of AUVs

Since the last decade, technological advancement has motivated the researchers towards the formation control of multiple AUVs. Better acoustic sensors and communication modules are developed which allow an AUV to interact with environment and with another AUV. In formation control, a fixed geometrical shape is maintained by AUVs as the objective is demanding. Like for mine countermeasure, all AUVs should move parallel to each other to collect as much data as possible in a single scan. These formation structures

can be decided by a leader in a leader-follower approach or it may be a group decision in a behavior approach. Generally the motion of multiple AUVs can be categorized under centralized and de-centralized technique.

A centralized system requires a large amount of data on navigation to be processed by a single unit. This unit may be a leader in a formation group or a surface ship which is monitoring some group of AUVs. But in a centralized technique, due to huge bi-directional data transfer, the usage of this technique is limited in real-world and also the guidance of multiple AUVs in a difficult environment will be a tough task. Whereas in decentralized technique there is no central processing unit and each vehicle has its own independent controller. Here, the AUVs have the ability to sense the environment and act on their own, which significantly reduces the cost of communication as in centralized technique. But still the large amount of data transfer exist between the AUVs.

In this thesis, a centralized approach for formation control is considered because centralized approach provides less complexity for small number of AUVs. Many researchers are developing and enhancing the control techniques for formation control. Some of the generally accepted control techniques for both centralized and decentralized methods are summed as follows

- Potential and Behavior based approach: In formation control the Behavior-based approach and potential field approach are considered for various applications. The basic principle behind behavior based approach is that,each AUV consists of a basic structure called motor schemas [17]. Each motor schemas generates its corresponding desired behavior, some of the motor schemas are collision avoidance, formation shape and goal seeking. The control input for a AUV is generated by weighted average of every motor schemas, thus a proper gain is adjusted using optimization technique. Few investigations [18, 19, 20] where initial applications of behavior based control are shown.

- Leader-Follower approach:Another approach uses leader-follower patterns in formation control. It is assumed that only local sensor based information is available for each AUV. There are two types of feedback controllers for maintaining formations of multiple AUVs. The leaders track predefined reference trajectories and the followers track transformed versions of the states of their nearest neighbors according to given schemes.

- Virtual Structure method:The concept of virtual structure was first introduced in [21]. The virtual structure approach is usually used in spacecraft or small satellite formation flying control [22]. Control methods are developed to force a group of agents to behave in a rigid formation. In virtual structure approach, the controller is

derived in three steps. First, the desired dynamics of the virtual structure is defined. Second, the desired motion of the virtual structure is translated into desired motions for each agent. Finally, individual tracking controllers for each agent are derived for agent tracking. In [14], the virtual structure method is combined with the leader-following method and behavioral approach to formation control of multiple spacecraft interferometer in deep space. In the virtual structure approach, the entire formation is treated as a single entity. When the structure moves, it traces out the desired trajectories for each robot in the group to track.

- Synchronization Based Control: In this method independent paths are derived from the desired path for each autonomous vehicle. These paths act as the desired paths but the motion of vehicle while following the respective paths should be coordinated. In other words, it can be said that there exists a velocity and acceleration constraint on each derived path. [23, 24, 25] are some of the works where synchronization approach has been applied for formation of mobile robot and surface vehicles.

1.5 Motivations

The development of control law for an AUV is complex and more challenging because the AUV is an underactuated system. Also the dynamics of AUV is very much influenced by the external environment. With the huge application of AUV in various fields and amongst them the path following is an basic requirement for every application.

As discussed earlier, the multiple AUVs as compared to single vehicle has better robustness towards vehicle failure and also has better data collection. For many time critical missions such as military operation or rescue missions, the use of multiple vehicles shows better performance as comparison to a single AUV.

1.6 Objectives of the Thesis

The objectives of the thesis are as follows.

- To develop a controller for an AUV considering thruster force and rudder plane as control input. These control input when supplied to dynamical equation, will steer the AUV towards the desired path. During the course of path following while maintaining the desired surge velocity.
- To develop a controller which will drive multiple AUVs towards a desired path or goal, while maintaining a desired shape. The controller will generate the desired surge and yaw velocity for the followers which allows them to follow the leader AUV maintaining the distance and orientation.

- Development of a graphical platform for visualizing the motion of an AUV and multiple AUVs in an ocean environment.

1.7 Problem Statement

1.7.1 Path following

The objective of the path following problem is to design a control law which will steer the AUV towards following the desired path. A path following controller for an underactuated AUV is to be designed to track the desired path while maintaining a desired constant velocity in the forward motion.

1.7.2 Formation control

Assuming that the information of the desired path is known to the leader AUV, and the follower AUV should follow the leader while maintaining a particular distance in both position and orientation. A control strategy is to be developed which enables the follower AUVs to follow the leader and also to maintain a fixed formation structure while in cooperative motion.

1.8 Thesis Organization

The thesis is organized as follows.

- Chapter 2 presents a literature survey on control methods of single AUV and multiple AUVs. Studies have been made on different control strategies reported in literature for pathfollowing. Also for achieving, successful cooperative motion, different control strategies are reported in literature are reviewed.

- Chapter 3 presents development of a control strategy using the concept of backstepping and fuzzy logic controller for path-following of an single AUV in x-y plane. The motion along surge, sway and yaw is considered and other motion related to depth and roll are neglected. In this chapter, the coupling of rudder angle between sway and yaw is also taken into consideration.

- In Chapter 4, the backstepping control technique for single AUV has been extended for obtaining formation control for multiple vehicles. In this chapter, the leader-follower formation strategy is adopted and assuming that only leader has the information about the path and follower follows the leader. This chapter also implements a fuzzy logic controller for leader-follower formation control. The result of both the controller have been presented and discussed.

- In Chapter 5, simulation on graphical interface of AUV motion control for both path following and formation control are discussed. The graphical visualization is created with the help of virtual-reality in SIMULINK 3D for better visualization of motion of single AUV or multiple AUVs in an ocean environment. This chapter also discusses about the selection of various hardware elements essential for the development and construction of an AUV.
- Chapter 6 concludes the thesis. Scopes of extension of present work are also discussed.
- Appendix-A presents the dynamics and kinematics of the AUV. These equations are used for the development of control algorithm for path following and formation control.
- Appendix-B presents the AUV(INFANTE) parameters considered for implementation of the proposed control algorithms.

Chapter 2

Literature Review on Control of AUV

In the past two decades, the majority of research has been devoted in the fields of Autonomous Underwater Vehicle motion control. An accurate motion control strategy is very important, for application of AUVs in various applications such as discussed in Section 1.2. Different motion control strategies which are generally adopted for AUV are path following, way point tracking, trajectory and localization. These motion control strategies are chosen based on either mission requirement or on commercial requirement. This thesis is concerned with the development of path following control of AUV. In path following strategy, a predefined path is assigned to the AUV and the AUV controller generates a control law which steers and propels the AUV to move in the desired path. But for single AUV path following control there is less requirement of sensor information. Very often instead of using single AUV multiple AUVs are employed in a cooperative motion control framework. This chapter reviews the reported control techniques for both the path following control and Co-operative motion control of AUVs.

2.1 Literature Review on path-following of AUV

In order to achieve the path following control of an AUV, the error between the path parameters and AUV position and orientation need to be reduced to zero. For this the control inputs to the AUV are thruster force and orientation of rudder, stern plane. Also the complete dynamics of AUV is a nonlinear 6DOF equation of motion with coupled and nonlinear terms involving added mass, hydrodynamic damping and also external disturbances by environment. So it is difficult to achieve accurate path following by using linear controllers, but some investigations have considered the approximated 2^{nd} order linear equation of AUV for designing path following controllers. In [26] 2^{nd} order AUV model is approximated to 3^{rd} order equation with the inclusion of an extra degree and its parameters are identified by using Markov parameter. The approximated linear equation is derived with assumption in nonlinear equation and it is suitable for specific operating

points. There are also some investigations employing the [27] the feedback linearization method for path following control but the linearization method or linear controllers are suitable for particular operating point. So for highly coupled and nonlinear equations the nonlinear controllers are suitable. Various nonlinear controllers from [28, 29, 30] can be applied for developing path following controller considering the following nonlinear dynamics. A number of nonlinear controllers such as backstepping controller, sliding mode control, soft computing approach are studied and the investigations in this area are applied are discussed below.

Fuzzy Logic controllers and sliding mode controllers have been implemented for AUV pathfollowing [31, 32, 33]. In [31], a sliding surface is used to represent the error between desired path and AUV position and taking this error in to consideration a fuzzy controller has been implemented for generating the control input i.e. rudder orientation. In [32], a sliding mode controller is designed for marine vessel but equations of motion are for 3dof which are considered for underwater vehicle. The marine vessel which is considered in [32] is considered to be fully actuated vehicle and in this literature the stability analysis was made using the Lyapunov method.

Another nonlinear controller which is mostly used for the autonomous vehicles is Backstepping controller, a Lyapunov based controller. An initial work on path tracking of mobile robots using the backstepping control is reported in [34]. Usually a mobile robot can be accurately controlled with the kinematics only but in the case of AUV only kinematics control is not sufficient because of nonlinearity and presence of coupling terms in the dynamics equation. In case of AUV, both the parameters of kinematics and dynamics need to be controlled. The backstepping control has been applied to AUV considering the complete dynamics equation in [2, 35, 36, 1] .

Referring [2], presents a path following control of an AUV by assuming a virtual vehicle that follows the desired path and the error between its position and orientation has been considered with backstepping controller. The boundedness and stability properties of the error backstepping is also presented in [2]. A similar approach has been applied for the path following problem of AUV [35, 36] with an exception that a Serret-Frenet frame is considered in place of virtual vehicle. But in the development of the pathfollowing controllers in [35, 36] the information for jerk parameter is required for effective path following but in practical cases the measurement of jerk parameter is difficult to measure. As this data is not available using any sensor so the controller heavily relies on mathematical model, but if parameter uncertainty mathematical model is considered then the jerk data will be an erroneous data. In [25], the S-F frame has been considered and problem of requests jerk information has been resolved. The [1] considers the dynamics of surface vessel which will be similar to AUV in 3DOF, but it assumes that the vessel

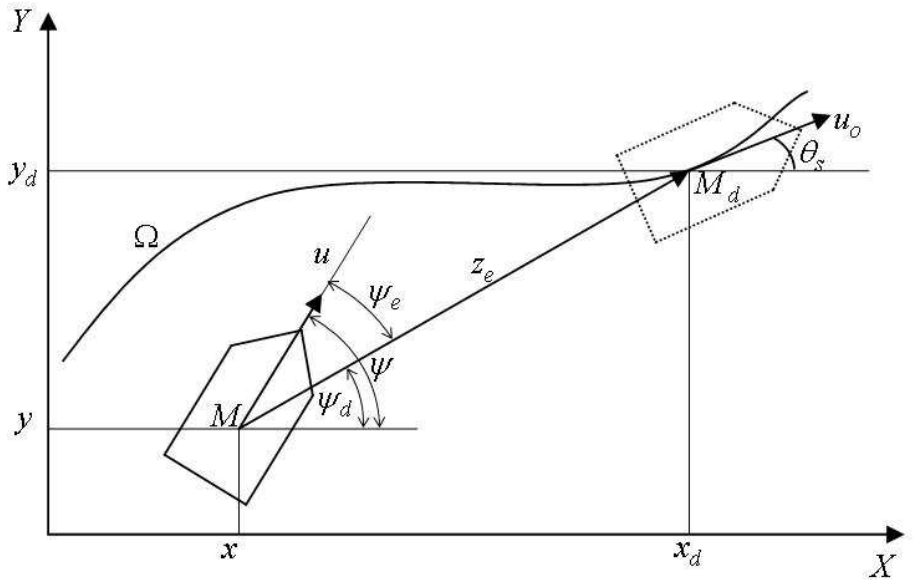

Figure 2.1: General framework of ship path following[2]

is moving with constant forward velocity. Also the coupling term of rudder control plane δ_r in the sway equation of motion is neglected. But when an AUV carries an unbalanced payload then this term cannot be neglected because the unbalanced payload will affect the coupling coefficient and the coefficient of the rudder control plane in sway will be large. These shortcomings are addressed in 3 during the development of path following controller.

2.2 Literature Review on cooperative motion of AUVs

Cooperative motion control refers to the collective behavior of multiple vehicles deployed for the fulfillment of a common mission for example survey operation. The other forms of cooperative motions are formation, flocking and swarming. The flocking and swarming approach is directly inherited from the motion of ants, birds etc but in the formation approach, multiple vehicles moves by maintaining a fixed geometrical structure. For implementation of formation control strategies for mobile robots, aerial vehicles and underwater vehicles various control strategies such as Leader-Following, Virtual structure based and behavior based strategies have been reported. Some of the early works on formation control focussed on mobile robots but subsequently with the development of improved sensors and actuators these methods can be applied to aerial vehicles and underwater vehicles.

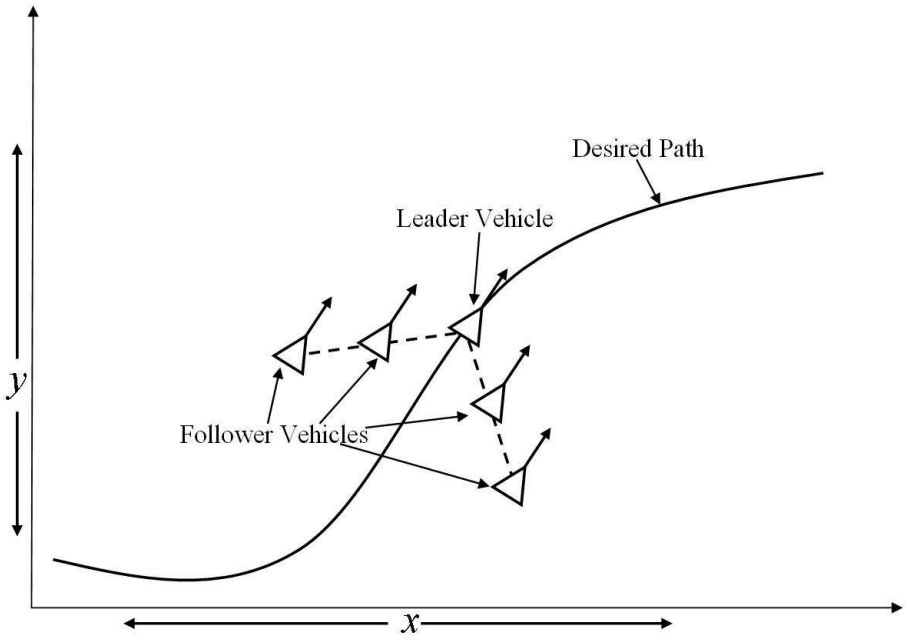

Figure 2.2: Illustration of wedge formation of Leader-Follower structure

2.2.1 Leader-Follower Control

The leader-follower strategy was first introduced by a German economist Heinrich Freiherr von Stackelberg. For addressing the multiple criteria, multiple decision making problems in economics.This leader-follower strategy is also known as Stackelberg strategies, later on this strategy finds wide application in formation control of multiple vehicles. In this strategy, the followers control laws depend upon the states of leader vehicle. The structure of leader-follower formation is shown in Fig.2.2, where multiple vehicles follow the desired path by maintaining a wedge like shape. During this formation, the followers have to follow the leader and avoids the collision with the neighbor vehicles or obstacles. This leader-follower strategy has been applied for formation of aerial, terrestrial as well as underwater vehicles. Due to interdependence of follower vehicle on leader vehicle, the information transfer of position and velocities is more.

In leader-follower approach, each vehicle is positioned with respect to the neighbor vehicle to form an geometrical structure. In a leader-follower strategy there are global leaders and also a local leader, for a particular formation group there is a single leader but the formation may have multiple local leaders. Referring to Fig.2.2, the vehicles next to leader vehicle will also be the local leader for the next corresponding vehicles. Among multiple vehicles, the global leader has the information about the path trajectory. This control structure is proposed in [37, 38, 39] for multiple mobile robots. Also transition from one formation structure to another formation structure is also presented with the help of graph theory. Refer [40], the leader-follower approach is also applied to underwater

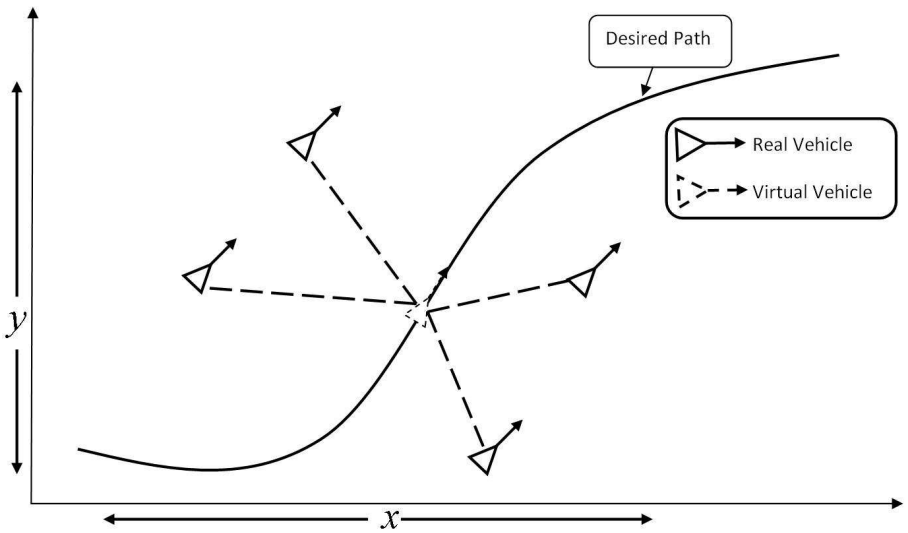

Figure 2.3: Example of virtual based formation control

vehicles. In this reference the dependence of follower AUV on leader states is addressed by the addition of a Neural Network function approximation, which will provide the approximate states of leader to the follower. [41] also adopts the similar approach where the estimator is used to estimate in the follower vehicle to estimate the velocity of the leader vehicle. [42, 43] implements sliding mode controller and fuzzy controller for developing a leader follower strategy among the vehicles.

2.2.2 Virtual Structure Based Control

Another approach towards formation control is Virtual Structure, where a imaginary rigid structure is assumed and the vehicles are connected to the respective nodes. This approach is identical to the leader-follower strategy but the difference lies in the physical presence of the leader vehicle. In virtual structure based approach, a virtual leader is considered, so the approach remains same for analysis. Similar to leader-follower approach the information of position and velocities of vehicles are to be regularly transferred. Thus, usually centralized method is adopted for implementation of virtual structure based strategy. Referring Fig.2.3, the virtual leader follows the desired path and the location of leader vehicle is transferred to other vehicles.

The virtual structure formation strategy adopts centralized approach but this approach can be modified for decentralized approach by assigning a virtual leader for each follower and a virtual leader position and orientation is calculated and communicated to each follower. The leader follower approach where the leaders position and orientation are independent of follower vehicles results increased actuation signal. But for virtual structure the leaders position and orientation are calculated from followers so perfect formation

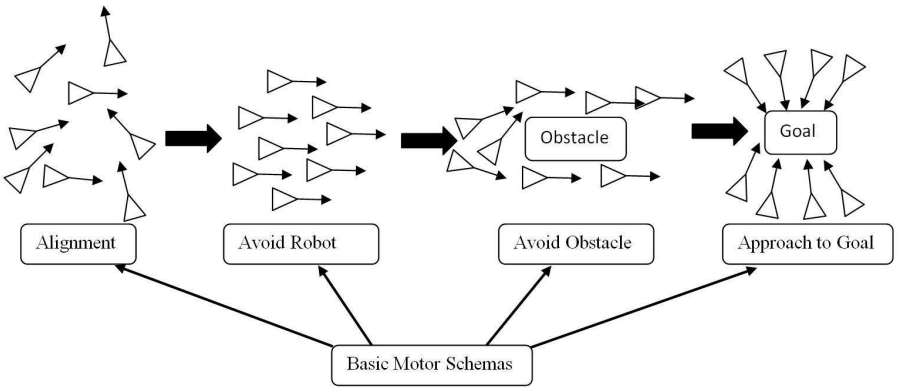

Figure 2.4: An example of motor schemas

structure can be guaranteed and also the less actuation signal requires to maintain the formation. This strategy is first introduced by [21], the principle behind the the approach is that the vehicles will move in such a way that the structure will move smoothly along the path. [44],[45] are some of the literatures where virtual structure approach is applied in mobile robots. An illustrative of virtual structure is represented in Fig.2.3. The advantages of virtual structure is that it is simpler to describe the coordination of multiple vehicles. Whereas the disadvantages with the virtual structure is that it limits the potential application where formation shape is time varying or when regular configuration is required.

2.2.3 Behavior Based Formation Control

The basic idea behind the concept of behavior based formation control[30] is to assign set of desired behaviors to each vehicles and the net control action will be the weighted average of each behavior. Here the behavior refers to the collision avoidance, goal following and formation keeping etc. In the literatures [20, 17, 46, 18] these behaviors are termed as motor schemas or functions. Unlike the leader-following formation control and virtual structure approach, less information needs to be communicated among the vehicles. But in the later to show the global convergence of the vehicles towards the desired goal is difficult.

From Fig.2.4, it is clear that the behavior based approach is influenced from the behavior of ants and bees. Refereing to [17] these kinds of flocking algorithms consist of simple motor schemas at individual level with some level of intelligence embed into it. One such kind of motor schemas is shown in Table.2.1. These motor schema provide the basic structure for moving towards the target and avoiding the obstacles. Here each motor schema provides a vector component according to the sensory input and a gain parameter represents the importance of the particular schema. A combined behavior is generated

Table 2.1: Motor Schemas Parameters for Formation Navigation Experiments in Simulation [17]

Parameter	Value	Units
Avoid-static-obstacle		
Gain	1.5	
Sphere of influence	50	meters
Minimum range	5	meters
Avoid-robot		
Gain	2.0	
Sphere of influence	20	meters
Minimum range	5	meters
Move-to-goal		
Gain	0.8	
Noise		
Gain	0.1	
Persistence	6	time steps
Maintain-formation		
Gain	1.0	
Desired spacing	50	meters
Controlled zone radius	25	meters
Dead zone radius	0	meters

by summing and normalizing the result of each motor schema. In [20], these schemas are represented as different reactive rules such as path finding, map learning, boundary following and safe wandering. These reactive rules take the input from sensors such as compass, sonar and fed the output to the motors for robot movement. These behavior based approach have been applied in the field of cooperative motion of AUVs [20, 17, 46].

2.3 Chapter Summary

In this chapter, various control strategies for single AUV path following and cooperative motion of multiple AUVs are studied and analyzed. It summarizes various controllers implemented for successful implementation for AUV path following. For cooperative control of multiple AUVs, various strategies has been discussed and also the literatures on cooperative motion has been studied.

Chapter 3

Path following Control Strategy for an Individual AUV

3.1 Introduction

Autonomous navigation and path control of an AUV possess difficult control problem owing to the fact that AUVs are underactuated systems i.e.the control inputs are less than degree of freedom. Navigating an AUV along a desired path is quite a difficult task due to presence of external disturbances such as ocean disturbance and also exact AUV parameters are unknown to the control engineers. The general navigational problems which are usually the active area of research are path following, trajectory tracking and waypoint tracking.

This chapter is organized as follows. In Section 3.3, we introduce the Serret-Frenet frame and its application in path following problem. The AUV kinematics and dynamics are discussed in Section 3.4.1 and Section 3.4.2. The error space between Serret-Frenet frame is given in Section 3.5 for the development of control algorithm. In Section 3.6, the control law is developed for successfully following a desired path. Finally the control algorithm is verified by simulations which are discussed in Section 3.7.

3.2 Objective

Let the desired path, P which the AUV is to follow Fig.3.1. It is intended to design a control law such that the AUV will follow the desired path P. Further the control of AUV is difficult due to underactuation. A path following controller for an underactuated AUV is to be designed such that it steers the AUV towards the desired path P while maintaining a constant velocity in the forward motion.

As per the objective the contribution of this chapter for addressing the path following problem are as follows.

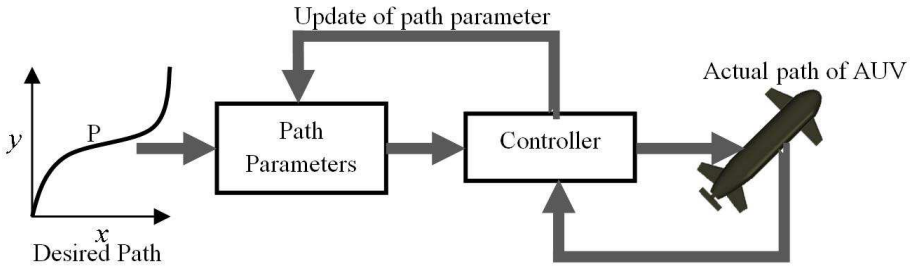

Figure 3.1: Path following controller implementation

- Developed the path following control considering the coupling of rudder angle between sway and yaw motion.
- Surge equation of motion is considered for achieving accurate path following.
- A graphical visualization is developed using Virtual Reality Modeling Language((VRML)) for analyzing the motion of AUV.

3.3 Introduction to Serret-Frenet Frame

Serret-Frenet Frame has been independently discovered by Jean Frdric Frenet in 1847 and Joseph Serret in 1851. Frenet presented an idea of attaching a frame at each point of the curve in space and as the frame moves along the curve the geometric parameters such as turn and twists can be determined. This theory of Frenet gives the six formulae of curve in space and Joseph Alfred Serret in 1851 contributed by giving all nine formulae of curve in space combining which makes Serret-Frenet Frame.

3.4 AUV Kinematics and Dynamics

Kinematics and dynamics of an AUV are described in Fig.3.2 where the transformation matrix T represents the transformation of body frame to earth fixed frame. The AUV parameter block represents the added mass and hydrodynamic coupled parameters. For implementing the path following control in x-y domain, only 3DoF is considered i.e. surge equation of motion is along x-direction, sway equation of motion is along y-direction and yaw equation of motion is angular movement along z-direction. The corresponding kinematic equations are also considered. For derivation and explanation of AUV kinematics and dynamics refer Appendix-A.

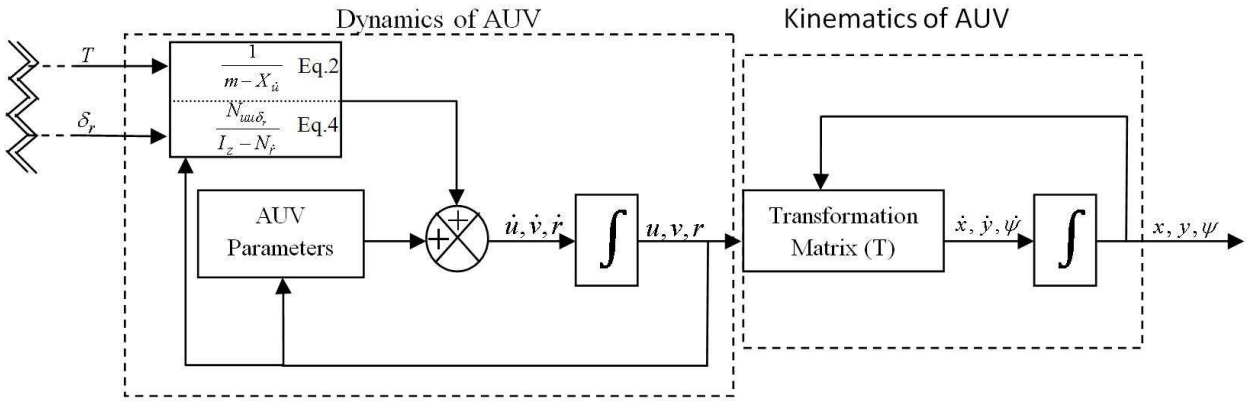

Figure 3.2: Kinematics and Dynamics structure of AUV

3.4.1 AUV Kinematics

The following are the kinematic equations for linear motion along x, y axes and rotational motion along the z axis.

$$\begin{aligned} \dot{x} &= u\cos(\psi) - v\sin(\psi) \\ \dot{y} &= u\sin(\psi) + v\cos(\psi) \\ \dot{\psi} &= r \end{aligned} \tag{3.1}$$

Here x, y are the linear positions whereas ψ is the angular position with reference to the Inertial frame I. u and v are the linear velocities of AUV along x-axis and y-axis and r is the angular velocity along z-axis.

3.4.2 AUV Dynamics

The motion of AUV along x-y plane is considered, and the components for motion contribution along z-axis are neglected i.e. heave and pitch equation of motion are neglected. The AUV considered in this work is a flat-fish type, so the roll equation of motion can be neglected. The following equations of motion are adopted from [3].
Surge Equation of Motion:

$$\dot{u} = \frac{m + X_{vr}}{m - X_{\dot{u}}} vr + \frac{X_{uu}}{m - X_{\dot{u}}} u^2 + \frac{T}{m - X_{\dot{u}}} \tag{3.2}$$

Sway Equation of Motion:

$$\dot{v} = -\left(\frac{m - Y_{ur}}{m - Y_{\dot{v}}}\right) ur + \frac{Y_{uv}}{m - Y_{\dot{v}}} uv + \frac{Y_{vv}}{m - Y_{\dot{v}}} v\,|v| + \frac{Y_{uu\delta_r} u^2 \delta_r}{m - Y_{\dot{v}}} \tag{3.3}$$

Yaw Equation of Motion:

$$\dot{r} = \frac{N_{vv}}{I_z - N_{\dot{r}}} v\,|v| + \frac{N_{rr}}{I_z - N_{\dot{r}}} r\,|r| + \frac{N_{ur}}{I_z - N_{\dot{r}}} ur + \frac{N_{uv}}{I_z - N_{\dot{r}}} uv + \frac{N_{uu\delta_r} u^2 \delta_r}{I_z - N_{\dot{r}}} \tag{3.4}$$

Table 3.1: Symbols used for Parameters of AUV

m	Mass of the vehicle
I_z	Inertial tensor in body frame B
$X_{\dot{u}}, Y_{\dot{v}}, N_{\dot{r}}$	Added mass of vehicle
$X_{uu}, Y_{vv}, N_{rr}, N_{vv}$	Cross-flow Drag
X_{vr}, Y_{ur}, N_{ur}	Added mass cross term and Fin lift
Y_{uv}, N_{uv}	Body lift force and Fin lift

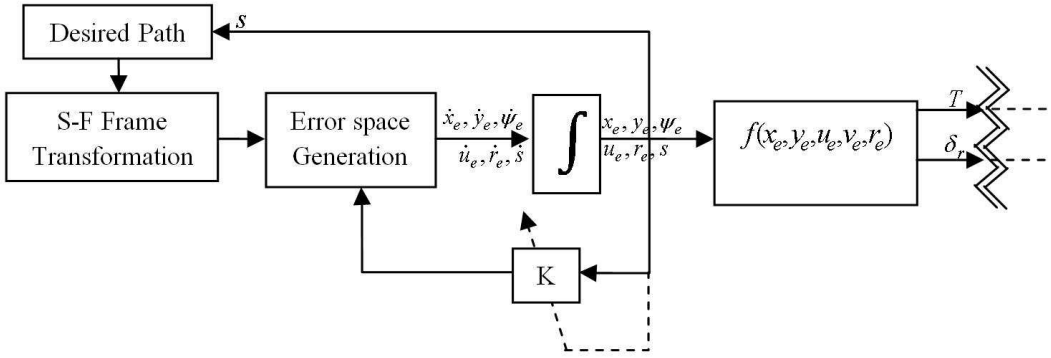

Figure 3.3: Control Structure for Path following

The symbols in the above equation of motion of the AUV are listed in Table 3.1:

The AUV dynamics (3.2)-(3.4) includes the thruster force T and rudder angle δ_r as control inputs. Here, it is clear that the equation of motion are coupled to each other and highly non-linear thus, development of controller for the AUV is challenging.

3.5 Development of Error Space

This Section contributes to the development of error space of AUV with in the Serret-Frenet frame. The error structure and notations used in this section are adapted from [1], [47]. Referring to Fig.3.3, the controller is to be designed to reduce the error generated in the error space. The control gains are adopted according to the error. Considering Fig.3.4, a desired path Ω is to be followed by an AUV with body frame $\{B\}$ attached to its center of gravity. A Serret-Frenet (S-F) frame is attached to a point S on the path. B is the point which can be described as $(x, y)^T$ in inertial frame $\{I\}$ or $(x_e, y_e)^T$ in S-F frame $\{F\}$, U is the net velocity of the AUV i.e. $U = \sqrt{u^2 + v^2}$, β is the angle between net velocity and sway velocity. $\theta_s$is the angle made by S-F frame with the inertial frame $\{I\}$ and $c_c$is the curvature at point S.

Referring [35] velocity at point S with reference to Inertial frame is expressed as following

$$v_S = v_B + R^{-1}\left(\frac{dBS}{dt}\right) + R^{-1}\left(\dot{\psi}_d \times BS\right) \tag{3.5}$$

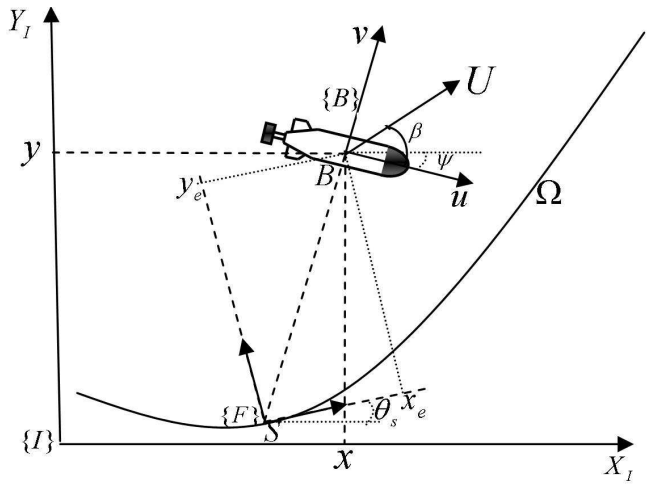

Figure 3.4: Representation of Serret-Frenet Frame Parameters

where

$$R = \begin{bmatrix} \cos(\psi_d) & \sin(\psi_d) & 0 \\ -\sin(\psi_d) & \cos(\psi_d) & 0 \\ 0 & 0 & 1 \end{bmatrix},$$

$v_S = [\dot{x}, \dot{y}, 0]^T$,

$Rv_B = [\dot{s}, 0, 0]^T$,

$\left(\frac{dBS}{dt}\right) = [\dot{x}_e, \dot{y}_e, 0]^T$,

$\dot{\psi}_d \times BS = [-c_c \dot{s} y_e, c_c \dot{s} x_e, 0]^T$.

v_S and v_B are the velocities at point S and B expressed in inertial frame I. ψ_d is the angle between a tangent at point S and x-axis of the Inertial Frame I, s is the arc length of the desired path Ω. c_c is the path curvature at point S. The position of AUV with reference to S-F Frame is x_e, y_e. Rewriting (3.5) by replacing the above defined parameters is

$$\begin{bmatrix} \dot{x}_e \\ \dot{y}_e \\ 0 \end{bmatrix} = R \begin{bmatrix} \dot{x} \\ \dot{y} \\ 0 \end{bmatrix} - \begin{bmatrix} \dot{s}\,(1 - c_c y_e) \\ \dot{s} c_c x_e \\ 0 \end{bmatrix} \tag{3.6}$$

For aligning the heading angle along the desired angle, the orientation error is defined as

$$\psi_e = \psi - \psi_d \tag{3.7}$$

and its derivative is

$$\dot{\psi}_e = r - c_c \dot{s} \tag{3.8}$$

The orientation error between total velocity U and $\dot{s}$ can be expressed as

$$\psi_e^* = \psi_e + \beta \tag{3.9}$$

where $\beta = \tan^{-1}(v/u)$ and ψ_e^* is described as the angular error between total velocity U and s of S-F frame. The following equations can be derived by rewriting the (3.6) in terms of ψ_e^*.

$$\begin{aligned} \dot{x}_e &= U\cos(\psi_e^*) - \dot{s}(1 - c_c y_e) \\ \dot{y}_e &= U\sin(\psi_e^*) - \dot{s}c_c x_e \end{aligned} \tag{3.10}$$

Differentiation of (3.9) gives,

$$\dot{\psi}_e^* = r + \dot{\beta} - c_c\dot{s} \tag{3.11}$$

3.6 Control Law Development

The error space developed in the previous section is considered here. Initially it is assumed that $\psi_e^* = \alpha_{\psi_e^*}$, where $\alpha_{\psi_e^*}$ is the angle that describes the desired orientation for AUV to follow the desired path. Consider a Lyapunov candidate function $V_1 = \frac{1}{2}(x_e^2 + y_e^2)$. Taking the derivative of the above Lyapunov equation, we have

$$\dot{V}_1 = (x_e\dot{x}_e + y_e\dot{y}_e) \tag{3.12}$$

and replacing $\dot{x}_e$ and $\dot{y}_e$ from (3.10) in (3.12), $\dot{V}_1$ is obtained as

$$\begin{aligned} \dot{V}_1 &= x_e\left(U\cos(\psi_e^*) - \dot{s}(1 - c_c y_e)\right) + y_e\left(U\sin(\psi_e^*) - \dot{s}c_c x_e\right) \\ &= x_e\left(U\cos(\psi_e^*) - \dot{s}(1 - c_c y_e)\right) + y_e\left(U\sin(\psi_e^*) - \dot{s}c_c x_e\right) \\ &= x_e U\cos(\psi_e^*) - x_e\dot{s} + U y_e\sin(\psi_e^*) \end{aligned} \tag{3.13}$$

It is assumed that the AUV initially moves such that it satisfies the condition i.e. $\psi_e^* = \alpha_{\psi_e^*}$. Replacing ψ_e^* with $\alpha_{\psi_e^*}$ then (3.13) is represented as

$$\begin{aligned} \dot{V}_1 &= x_e U\cos\left(\alpha_{\psi_e^*}\right) - x_e\dot{s} + U y_e\sin\left(\alpha_{\psi_e^*}\right) \\ &= x_e\left(U\cos\left(\alpha_{\psi_e^*}\right) - \dot{s}\right) + U y_e\sin\left(\alpha_{\psi_e^*}\right) \end{aligned} \tag{3.14}$$

It is straightforward that the following choice of the update rate i.e.

$$\dot{s} = U\cos(\alpha_{\psi_e^*}) + k_s x_e \tag{3.15}$$

yields

$$\dot{V}_1 = -k_s x_e^2 + U y_e\sin(\alpha_{\psi_e^*}) \tag{3.16}$$

and as $sign(y_e) = -sign(\alpha_{\psi_e^*})$ always holds, thus (3.16) is always a decreasing function.The desired orientation is to be designed such that the 2^{nd} term of $\dot{V}_1$ of (3.16) should always be a negative term, which leads to the complete convergence of $\dot{V}_1$ to zero. The choice of desired orientation should ensure that it is always differentiable at $t = 0$. Let this function can be selected as

$$\alpha_{\psi_e^*} = -\left(1 - e^{-t/\tau}\right)\theta_a \tanh\left(k_\delta y_e\right) \tag{3.17}$$

where τ is the smoothing factor for $\alpha_{\psi_e^*}$. Let the deviation from actual angular position (ψ_e^*) from the desired approaching angle ($\alpha_{\psi_e^*}$) be defined as $\bar{\psi}_e = \psi_e^* - \alpha_{\psi_e^*}$.
The derivative of $\bar{\psi}_e$ while following the desired path is as follows:

$$\dot{\bar{\psi}}_e = r + \dot{\beta} - c_c\dot{s} - \dot{\alpha}_{\psi_e^*} \tag{3.18}$$

From (3.18), if α_r is defined as the desired yaw velocity then actual yaw velocity r can be expressed as $r_e + \alpha_r$. Rewriting (3.18) with r replaced as $r_e + \alpha_r$ is

$$\dot{\bar{\psi}}_e = r_e + \alpha_r + \dot{\beta} - c_c\dot{s} - \dot{\alpha}_{\psi_e^*} \tag{3.19}$$

In terms of Backstepping method this new term α_r act as a control input for (3.19). The objective is to select the control input such that (3.19) gradually decreases to zero. Thus a Lyapunov function V_2 is considered which corresponds to the positive definite error function for minimizing the $\bar{\psi}_e$error.

$$V_2 = \frac{1}{2}\bar{\psi}_e^2 \tag{3.20}$$

For minimizing the orientation error, the derivative of the Lyapunov function (3.20) should gradually decrease to zero so that the AUV orientation gradually aligns to the desired orientation. Taking the derivative of above Lyapunov function,

$$\begin{aligned}
\dot{V}_2 =& \bar{\psi}_e\dot{\bar{\psi}}_e \\
=& \bar{\psi}_e\left(\frac{u}{U^2}\left(\frac{Y_{uv}}{m-Y_{\dot{v}}}uv + \frac{Y_{vv}}{m-Y_{\dot{v}}}\left|v\right|v + \frac{Y_{uu\delta_r}u^2\delta_r}{m-Y_{\dot{v}}}\right)\right. \\
&+ \beta r_e - \frac{v}{U^2}\left(\frac{X_{uu}}{m-X_{\dot{u}}}u^2 + \frac{T}{m-X_{\dot{u}}}\right) + \\
&\left. c_c\dot{s} + \dot{\alpha}_{\psi_e^*} + \beta\alpha_r\right)
\end{aligned} \tag{3.21}$$

and choosing the α_r as following

$$\alpha_r \quad = F_1 + F_2\delta_r + F_3T \tag{3.22}$$

where
$F_1 = \frac{-K_{\bar{\psi}_e}\bar{\psi}_e}{\beta} - \frac{u}{\beta U^2}\left(\frac{Y_{uv}}{m-Y_{\dot{v}}}uv + \frac{Y_{vv}}{m-Y_{\dot{v}}}\left|v\right|v\right) + \frac{v}{\beta U^2}\left(\frac{X_{uu}}{m-X_{\dot{u}}}u^2\right) + \frac{c_c\dot{s}+\dot{\alpha}_{\psi_e^*}}{\beta}$,
$F_2 = \frac{-u}{\beta U^2}\frac{Y_{uu\delta_r}u^2}{m-Y_{\dot{v}}}$,
$F_3 = \frac{v}{\beta U^2 m - X_{\dot{u}}}$.
by replacing α_r in (3.21), the derivative of Lyapunov function V_2 is expressed as following.

$$\dot{V}_2 = \bar{\psi}_e\beta r_e - K_{\bar{\psi}_e}\bar{\psi}_e^2 \tag{3.23}$$

The 2^{nd} term is a decreasing function where as the 1^{st} term consists of βr_e. If r_e reduces to zero then the Lyapunov function $\dot{V}_2$ gradually reduces to zero and the AUV will approach towards the desired orientation angle. The boundedness of r_e parameter is considered later in this chapter and

$$\beta = \left(1 - \frac{u^2}{U^2}\frac{m - Y_{ur}}{m - Y_{\dot{v}}} - \frac{v^2}{U^2}\frac{m + X_{vr}}{m - X_{\dot{u}}}\right) \tag{3.24}$$

which is always greater than zero and bounded.
Let u_d represents the desired surge velocity. The deviation from the desired surge velocity from the actual surge velocity can be expressed as follows

$$u_e = u - u_d \tag{3.25}$$

Taking derivative of surge velocity error u_e, we have

$$\dot{u}_e = \frac{m + X_{vr}}{m - X_{\dot{u}}} v r_e + \frac{m + X_{vr}}{m - X_{\dot{u}}} v\alpha_r + \frac{X_{uu}}{m - X_{\dot{u}}} u^2 + \frac{T}{m - X_{\dot{u}}} \tag{3.26}$$

Consider a Lyapunov candidate function V_3 which is a positive definite function of surge velocity error (u_e). One such Lyapunov function considered for V_3 is

$$V_3 = \frac{1}{2} u_e^2 \tag{3.27}$$

and taking the derivative of the Lyapunov function.

$$\dot{V}_3 = u_e \dot{u}_e \tag{3.28}$$

Replacing the term $\dot{u}_e$ from (3.26) into (3.28), the $\dot{V}_3$ is expressed as

$$\dot{V}_3 = u_e \frac{m + X_{vr}}{m - X_{\dot{u}}} v r_e + \frac{m + X_{vr}}{m - X_{\dot{u}}} v\alpha_r + \frac{X_{uu}}{m - X_{\dot{u}}} u^2 + \frac{T}{m - X_{\dot{u}}} \tag{3.29}$$

By selecting the control input T as

$$T = \frac{F_6}{F_4} - \frac{F_5}{F_4}\delta_r \tag{3.30}$$

where
$F_4 = \frac{1}{m - X_{\dot{u}}} + \frac{m + X_{vr}}{m - X_{\dot{u}}} v F_3$,
$F_5 = \frac{m + X_{vr}}{m - X_{\dot{u}}}$,
$F_6 = -K_{u_e} u_e - \frac{X_{uu}}{m - X_{\dot{u}}} - \left(\frac{m + X_{vr}}{m - X_{\dot{u}}}\right) v F_1$.
and replacing it with (3.29), then it becomes

$$\dot{V}_3 = \frac{m + X_{vr}}{m - X_{\dot{u}}} v r_e u_e - K_{u_e} u_e^2 \tag{3.31}$$

Where it is clear that the surge velocity error u_e approaches to zero only if the 1^{st} term is shown as bounded or decreasing function. From (3.31) and (3.23) it is observed that

the following Lyapunov function will approach to zero only if yaw error r_e reduces to zero or if it is a bounded function. Hence, considering the r_e error and taking its derivative of $r_e = r - \alpha_r$ i.e.

$$\dot{r}_e = \frac{N_{vv}}{I_z - N_{\dot{r}}} v\,|v| + \frac{N_{rr}}{I_z - N_{\dot{r}}} r\,|r| + \frac{N_{ur}}{I_z - N_{\dot{r}}} ur + \frac{N_{uv}}{I_z - N_{\dot{r}}} uv + \frac{N_{uu\delta_r} u^2 \delta_r}{I_z - N_{\dot{r}}} - \dot{\alpha}_r \tag{3.32}$$

and considering a Lyapunov function $V_4 = \frac{1}{2} r_e^2 + \frac{1}{2} u_e^2 + \frac{1}{2} \bar{\psi}_e^2$ for stabilization of yaw velocity error. Taking the derivative of the defined Lyapunov function which is

$$\dot{V}_4 = r_e \dot{r}_e + \dot{V}_2 + \dot{V}_3 \tag{3.33}$$

and replacing $\dot{V}_2$ and $\dot{V}_3$ from (3.23) and (3.31) the expression for $\dot{V}_4$ can be expressed as follows:

$$\dot{V}_4 = r_e \dot{r}_e + u_e \left(\frac{m + X_{vr}}{m - X_{\dot{u}}} v r_e - K_{u_e} u_e \right) + \bar{\psi}_e \left(\beta r_e - K_{\bar{\psi}_e} \bar{\psi}_e \right) \tag{3.34}$$

According to Lyapunov stability theory the derivative of the positive definite Lyapunov function should be a negative definite. So selecting a negative definite function as

$$\dot{V}_4 = -K_{r_e} r_e^2 + \left(\frac{N_{rr}}{I_z - N_{\dot{r}}} |r| + \frac{N_{ur}}{I_z - N_{\dot{r}}} u \right) r_e^2 - K_{u_e} u_e^2 - K_{\bar{\psi}_e} \bar{\psi}_e^2 \tag{3.35}$$

In this expression the gain parameter is always considered as positive quantity and the AUV dynamic equation parameter $\left(\frac{N_{rr}}{I_z - N_{\dot{r}}} |r| + \frac{N_{ur}}{I_z - N_{\dot{r}}} u \right)$ in the AUV dynamic equation is always a negative quantity(refer Appendix 2). So it is clear that the error parameter of angular velocity r_e reduces to zero and it is shown that $(x_e, y_e), \psi_e, u_e$ and r_e converges to zero exponentially. Equating Equations (3.34) and (3.35) the following condition holds

$$T F_7 + \delta_r F_8 - \dot{\alpha}_r = F_9 \tag{3.36}$$

where

$F_7 = F_3 \left(\frac{N_{rr}}{I_z - N_{\dot{r}}} |r| + \frac{N_{ur}}{I_z - N_{\dot{r}}} u \right) - K_{r_e} F_3,$

$F_8 = \frac{N_{uu\delta_r} u^2}{I_z - N_{\dot{r}}} + F_2 \left(\frac{N_{rr}}{I_z - N_{\dot{r}}} |r| + \frac{N_{ur}}{I_z - N_{\dot{r}}} u \right) - K_{r_e} F_2,$

$F_9 = K_{r_e} (F_1 - r) - \beta \bar{\psi}_e - \left(\frac{m + X_{vr}}{m - X_{\dot{u}}} \right) u_e v - \left(\frac{N_{rr}}{I_z - N_{\dot{r}}} |r| + \frac{N_{ur}}{I_z - N_{\dot{r}}} u \right) F_1 - \frac{N_{uv}}{I_z - N_{\dot{r}}} uv - \frac{N_{vv}}{I_z - N_{\dot{r}}} |v|\, v.$

On solving (3.30) and (3.36), the desired value of thruster force and rudder angle can be generated for successfully following the desired path.

Simplification of α_r: Recalling the value of $\alpha_r = F_1 + F_2 \delta_r + F_3 T$ and by replacing the expression of Thrust from ((3.30)), then α_r is expressed as:

$$\alpha_r = F_1 + \frac{F_3 F_6}{F_4} + \delta_r \left(\frac{-u Y_{uu\delta_r} u^2}{\beta U^2 m - Y_{\dot{v}}} \right) \left(1 - \frac{m + X_{vr}}{m - X_{\dot{u}}} \frac{v^2}{\beta U^2} \right) \tag{3.37}$$

As $\frac{Y_{uu\delta_r}}{m - Y_{\dot{v}}} << 1$ so neglecting the coefficients of δ_r, α_r and replacing $F_i : (i \in [1, 6])$ ((3.37)) can be represented as follows:

$$\alpha_r = \frac{-K_1 \bar{\psi}_e}{\beta} - \frac{u}{\beta U^2} \left(\frac{Y_{uv}}{m - Y_{\dot{v}}} uv + \frac{Y_{vv}}{m - Y_{\dot{v}}} |v|\, v \right) - \frac{K_{u_e} u_e v}{\beta U^2} + \frac{c_c \dot{s}}{\beta} + \frac{\dot{\alpha}_{\psi_e^*}}{\beta} \tag{3.38}$$

Unlike in [1], $\dot{\alpha}_r$ has been obtained using the partial derivative of α_r. Addition of surge motion increases the parameters involved in α_r, So it becomes difficult for finding $\dot{\alpha}_r$ through partial derivative. A simpler procedure of applying a high pass filter with appropriate cut-off frequency because high pass filter can act as a differentiator. The cut-off frequency and order of the filter is varied till the filter output is similar to the mathematical model of $\dot{\alpha}_r$. Out of many possibilities, the following is one of the filter model which act as differentiator for our problem. The filter chosen as 2^{nd} order high-pass Butterworth filter with cut-off frequency $1Hz$ is.

$$\begin{aligned} \dot{x} &= \begin{bmatrix} -8.85 & -39.47 \\ 1 & 0 \end{bmatrix} x + \begin{bmatrix} 1 \\ 0 \end{bmatrix} u \\ y &= \begin{bmatrix} -8.85 & -39.47 \end{bmatrix} x + u \end{aligned} \tag{3.39}$$

Controller Gain Update Rule:

The rate of change of gain is directly proportional to the corresponding error terms and $\sigma_i, \alpha_i : i(1...n)$ are considered as small positive constants. Here n is the number of controller gains available for tuning.

$$\begin{aligned} \dot{K}_{\bar{\psi}_e} &= -\sigma_1 K_{u_e} + \alpha_1 \left(\bar{\psi}_e^2\right) \\ \dot{K}_{u_e} &= -\sigma_2 K_{u_e} + \alpha_2 \left(u_e^2\right) \\ \dot{K}_{r_e} &= -\sigma_3 K_{r_e} + \alpha_3 \left(r_e^2\right) \\ \dot{K}_s &= -\sigma_4 K_s + \alpha_4 \left(s^2\right) \end{aligned} \tag{3.40}$$

Boundedness of β:

Rewriting the term β from (3.24) is

$$\beta = \left(1 - \frac{u^2}{U^2}\frac{m - Y_{ur}}{m - Y_{\dot{v}}} - \frac{v^2}{U^2}\frac{m + X_{vr}}{m - X_{\dot{u}}}\right) \tag{3.41}$$

Let $x_1 = \frac{u^2}{U^2}\left(\frac{m-Y_{ur}}{m-Y_{\dot{v}}}\right)$ and $x_2 = \frac{v^2}{U^2}\left(\frac{m+X_{vr}}{m+X_{\dot{u}}}\right)$ are the two functions then rewriting the terms following the property $A.M \geq G.M$ will be as follows

$$\frac{\frac{u^2}{U^2}\left(\frac{m-Y_{ur}}{m-Y_{\dot{v}}}\right) + \frac{v^2}{U^2}\left(\frac{m+X_{vr}}{m+X_{\dot{u}}}\right)}{2} \geq \sqrt{\frac{u^2}{U^2}\left(\frac{m - Y_{ur}}{m - Y_{\dot{v}}}\right)\frac{v^2}{U^2}\frac{m + X_{vr}}{m + X_{\dot{u}}}} \tag{3.42}$$

replacing the numerator term of A.M with β the above inequality can be written as

$$\frac{1 - \beta}{2} \geq \frac{uv}{U^2} \tag{3.43}$$

and after rearranging the inequality is represented as following

$$\beta \leq \frac{(u - v)^2}{U^2} \tag{3.44}$$

As it is a path following problem so at surge velocity(u) will not be zero at any point of time and from the inequality it is clear that β will never be zero and is bounded quantity.

Table 3.2: Infante AUV Hydrodynamic parameter [3]

m=2234.5kg	I_z=2000 N.m.s^2
$X_{\dot{u}}$=-141.9 kg	X_{uu}=-35.4 kg/m
$Y_{\dot{v}}$=-1715.4 kg	Y_{vv}=-667.5 kg/m
$N_{\dot{r}}$=-1349 kg.m^2/rad	N_{rr}=-310
N_{vv}=433.8 kg	X_{vr}=1715.4 kg/rad
Y_{ur}=103.4 kg/rad	N_{ur}=-1427 kg.m/rad
Y_{uv}=-346.76 kg/m	N_{uv}=-686.08 kg

Table 3.3: Controller gain parameters

σ_1=0.01	α_1=0.02
σ_2=0.04	α_2=0.08
σ_3=0.01	α_3=0.08
σ_4=0.04	α_4=0.4

3.7 Results and Discussions

Simulations are performed using MATLAB for verifying the performance of backstepping control law for steering the AUV to desired Serret-Frenet frame path. For the above simulations, AUV parameters used as given in Table 3.2[3]. The parameters for updating the controller gains are given in Table 3.3. The initial conditions for simulation are taken as $[s, x, y, \psi, u, v, r, k_1, k_2, k_3] = [0, 0, 0, 0, 0.5, 0, 0, 0, 0, 0]$. Fig.3.5 and Fig.3.6 show the the AUV position and orientation while following the desired circular path. The error between AUV position and Serret-Frenet frame is plotted in Fig.3.7. As the initial distance is more between S-F frame and AUV, so the update rate shown in Fig.3.8 initially increases and then maintains a uniform update rate. While following the circular path, the variation of surge and sway velocities are shown in Fig.3.9 and Fig.3.10. The yaw velocity is shown in Fig.3.11. For maintaining the desired velocity i.e. $u_d = 1$ and traversing the path, the controller of AUV generates the desired thruster force and rudder angle. Fig.3.12 and Fig.3.13 show the thruster force and rudder angle required while following the circular path. According to the error in position and orientation the controller gains are adjusted and is shown in Fig.3.14. The effectiveness of the derived controller has been compared with controller developed in [1]. Fig.3.16 compares the effectiveness of the derived controller and [1]. From the figure it is clear that the developed control algorithm results better performance because the surge motion dynamics is introduced and the adaptive control gains are implemented. Initially the error between the origin of the desired path and AUV frame is more and gradually as AUV approaches to the path the error should be decreasing, this result is shown in Fig.3.16. Fig.5(a) also demonstrates the comparison between the generated rudder input from the respective control algorithms. For the same path the control actuation differs, the controller actuation with lesser variation shows less power consumption. It is clear that the developed control algorithm performs better than

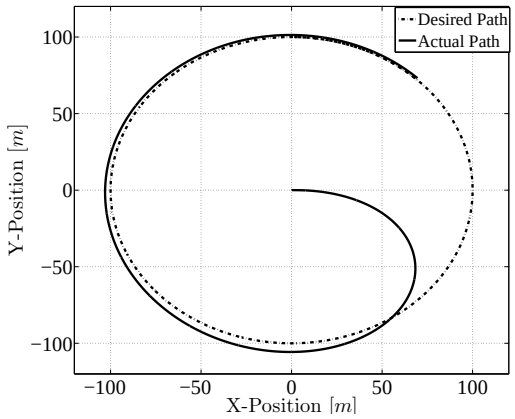

Figure 3.5: AUV Following a desired circular path

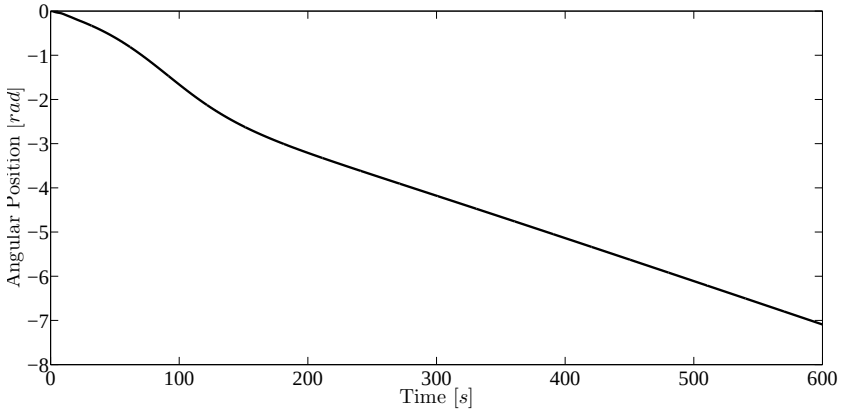

Figure 3.6: Angular Position of AUV while traversing the circular path

Table 3.4: Comparison of control algorithms

Comparison	Reaching Time(sec)	Rudder Variation(rad)
Ghommam et.al	≈ 1500	$min = -0.51, max = 0.99$
Developed Algorithm	≈ 600	$min = -0.06, max = 0.66$

the control algorithm presented in [1]. Table 3.4 shows the comparison of two control algorithms on the basis of reaching to the path and variation of rudder input.

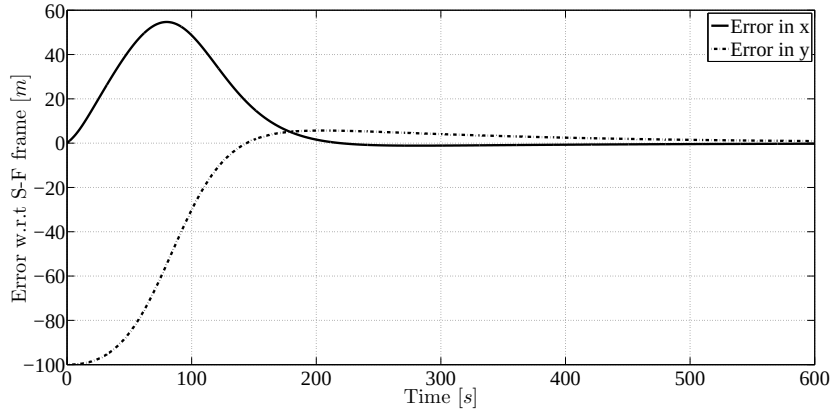

Figure 3.7: Distance error between AUV and S-F frame

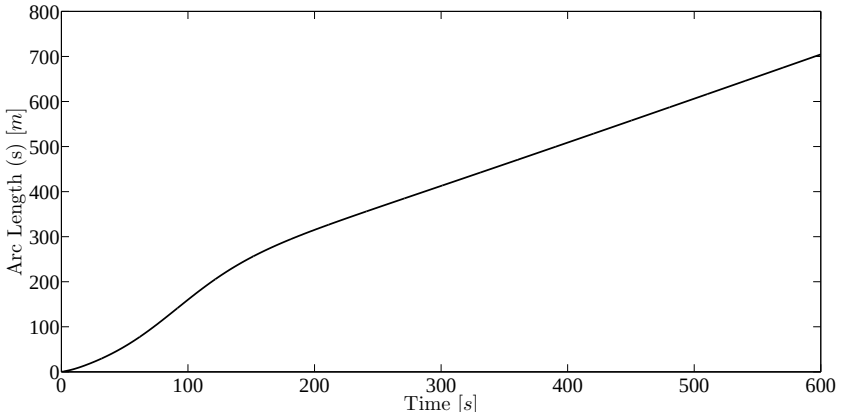

Figure 3.8: Represents the update rate of S-F frame along the circular path

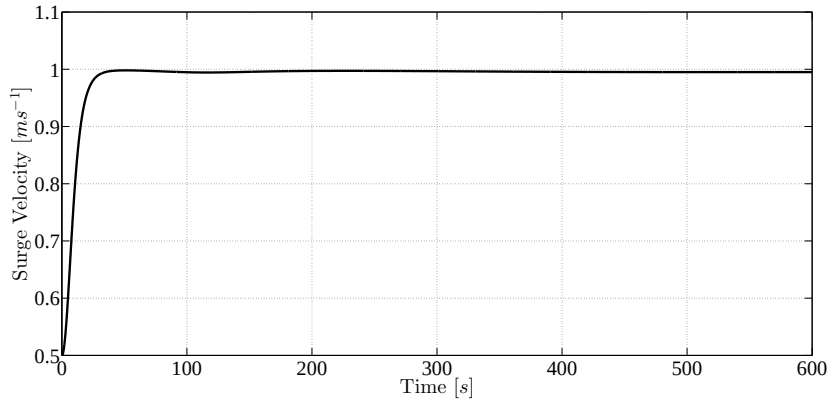

Figure 3.9: Variation of Surge velocity along the path

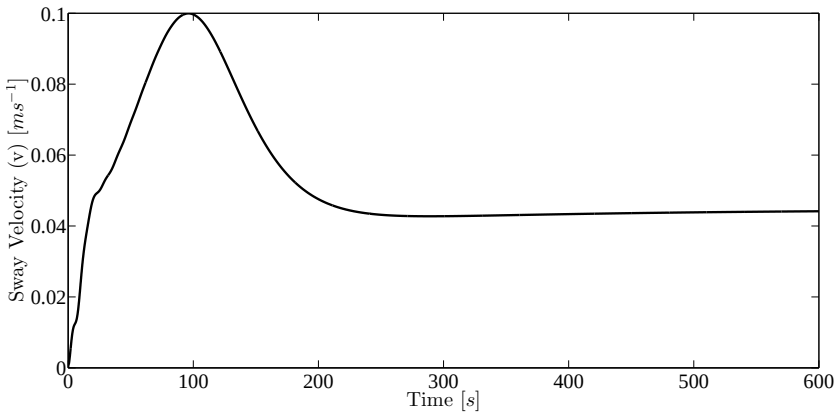

Figure 3.10: Variation of Sway velocity along the path

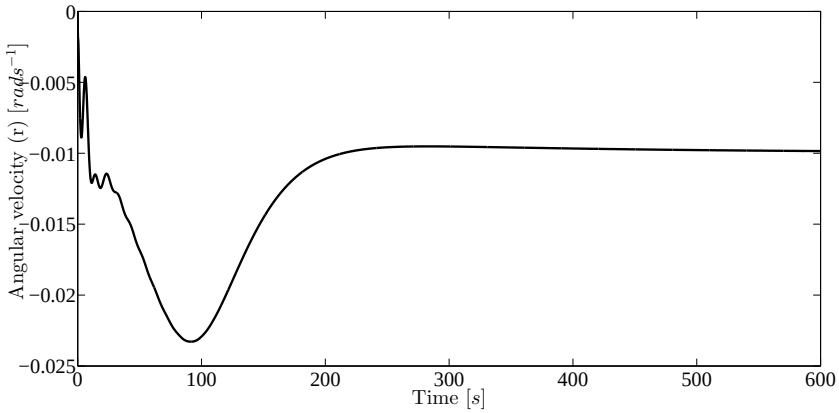

Figure 3.11: Variation of Yaw velocity along the path

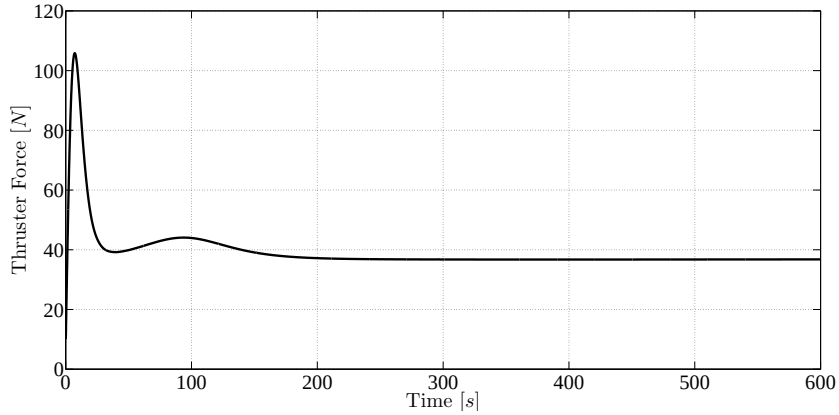

Figure 3.12: Thruster variation with respect to time

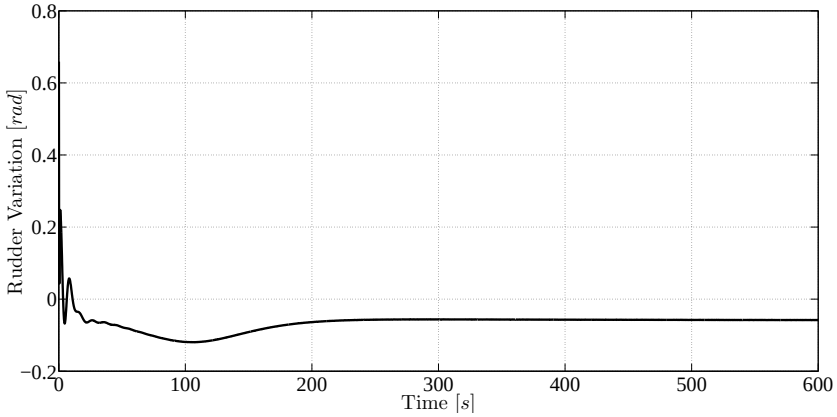

Figure 3.13: Rudder Variation with respect to time

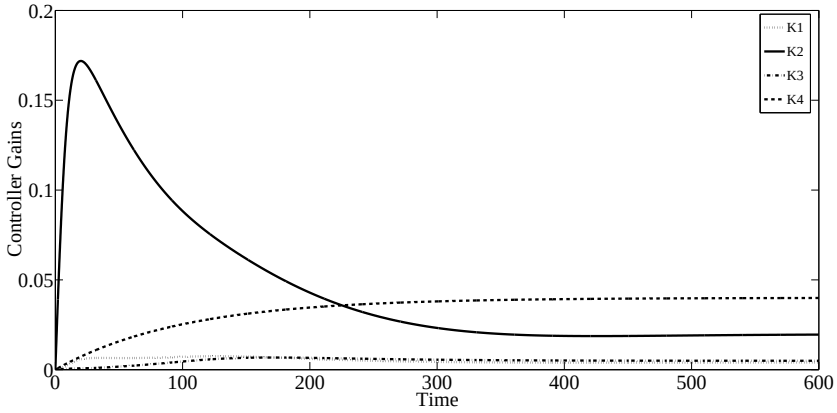

Figure 3.14: Controller gain update with respect to time

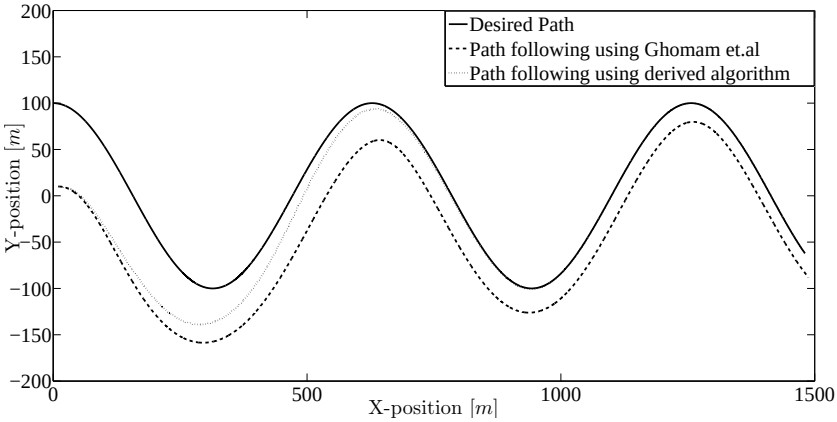

Figure 3.15: Comparison of path following control of an AUV along the desired path

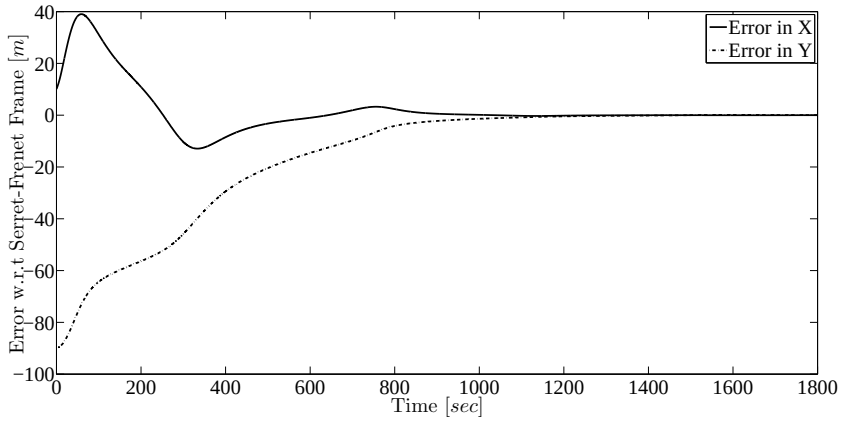

Figure 3.16: Error between the path and desired path

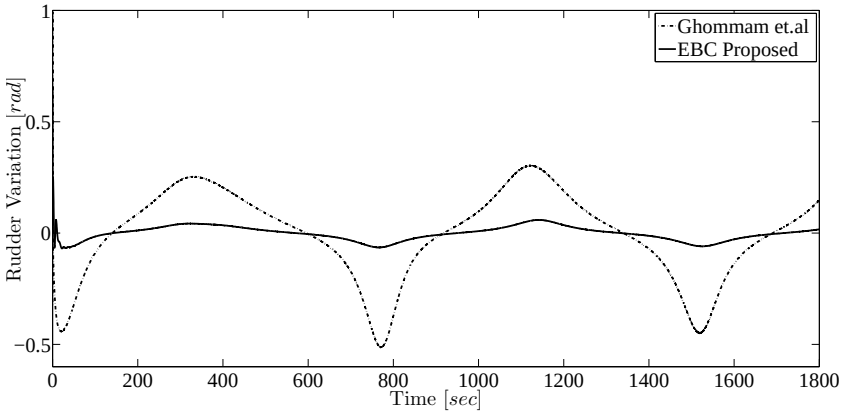

Figure 3.17: Comparison of Rudder variation of the AUV while traversing the path

3.8 Chapter Summary

In this chapter, a Lyapunov based backstepping approach to design an adaptive path following control of an AUV is developed considering both kinematics and dynamics. Here, Serret-Frenet frame approach for path following is chosen and a Lyapunov positive definite function is chosen for minimizing the corresponding error in position and orientation and from there using backstepping method a control law is derived which drives the AUV to the desired S-F frame.

Chapter 4

Formation Control of Multiple Autonomous Vehicles

4.1 Introduction

Formation control of multiple AUVs is an challenging research topic among many researchers. Recently the research interests are increasingly employing towards multiple AUVs because robustness is achieved in the mission to handle situations such as single vehicle failure and also use of multiple vehicle reduces the amount of work by single vehicle. For many applications such as surveillance, mine counter measure instead of single AUV, a group of AUVs are deployed to follow a desired path while maintaining an assigned geometrical shape. In brief, the formation control is referred as controlling the relative position and orientation of a number of AUVs in a group while the group as a whole follows a desired path.

This chapter is organized as follows. The kinematics and dynamics of leader and follower AUV are discussed in Section 4.3. This chapter is composed of two formation controller, Section 4.4 develops the formation control using backstepping control strategy and Section 4.5.1 using fuzzy logic controller. The error space is developed between Leader and Follower AUV in Section 4.4.1 for the development of formation control law. In Section 4.4.2, a formation control law for Follower AUV is developed for successfully following the Leader AUV, whereas the Leader AUV follows the desired path as discussed in the previous chapter 3. Finally the effectiveness of the above developed control algorithm is verified by pursuing simulation studies and are presented in Section 4.6. This chapter concludes with summary in Section 4.7.

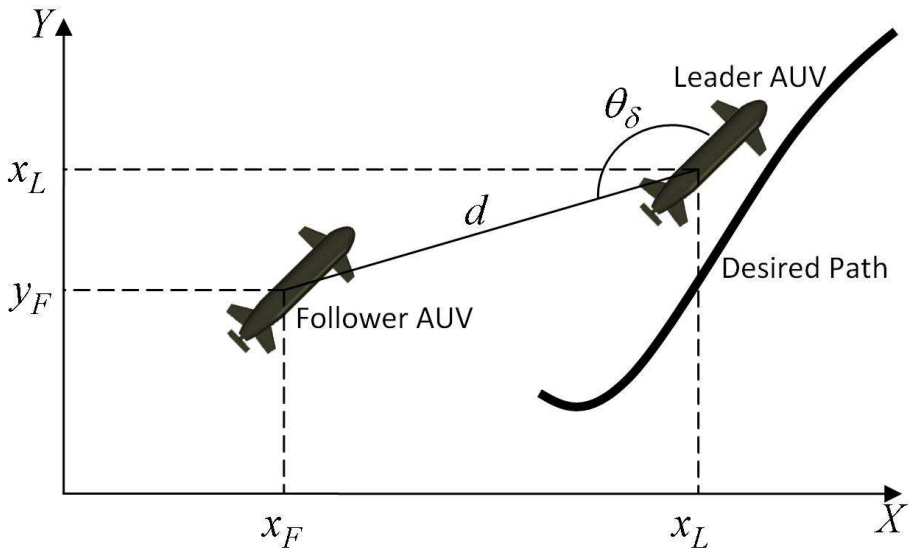

Figure 4.1: Leader-Follower Formation structure

4.2 Problem Statement

Let the desired path is known to the leader AUV, and the follower AUV should maintain a particular distance in both position and orientation. The control design for leader AUV is implemented as discussed in the previous chapter 3. A general approach for leader follower formation is shown in Fig.4.1, where follower should follow the leader along with maintaining a particular distance from the leader and also with a desired orientation from the leader. During the development of control law, we assumed that the cooperative motion is restricted in x-y plane.

4.3 Kinematics and Dynamics of Leader and follower AUVs

For formation control of multiple AUVs the kinematics and dynamics of the leader and follower AUV's are assumed to be same. But for the follower AUV, the rudder angle coupling between sway motion and yaw motion is not considered for simplicity. Thus, the kinematics and dynamics of the leader and follower AUVs are described as follows.

4.3.1 Leader AUV

The following are the kinematic equations for leader AUV along x, y axes and rotational motion along the z axis.

$$\begin{aligned} \dot{x_L} &= u_L \cos(\psi_L) - v_L \sin(\psi_L) \\ \dot{y_L} &= u_L \sin(\psi_L) + v_L \cos(\psi_L) \\ \dot{\psi_L} &= r_L \end{aligned} \tag{4.1}$$

where, x_L, y_L are the leader AUV position and ψ_L is the AUV angular position with reference to the Inertial frame I. u_L, v_L are the leader velocities along the surge and sway motion and r_L is the angular motion along yaw direction.
Assuming that the dynamics of AUV considered in previous chapter 3 is the same for the leader AUV. The following are the dynamics of the leader AUV,
The equation of motion along surge direction can be expressed as

$$\dot{u_L} = \frac{m + X_{vr}}{m - X_{\dot{u}}} v_L r_L + \frac{X_{uu}}{m - X_{\dot{u}}} {u_L}^2 + \frac{T_L}{m - X_{\dot{u}}} \tag{4.2}$$

The equation of motion along sway direction can be expressed as

$$\dot{v_L} = -\left(\frac{m - Y_{ur}}{m - Y_{\dot{v}}}\right) u_L r_L + \frac{Y_{uv}}{m - Y_{\dot{v}}} u_L v_L + \frac{Y_{vv}}{m - Y_{\dot{v}}} v_L |v_L| + \frac{Y_{uu\delta_r} {u_L}^2 \delta_r}{m - Y_{\dot{v}}} \tag{4.3}$$

The equation of motion along yaw direction is given by

$$\dot{r_L} = \frac{N_{vv}}{I_z - N_{\dot{r}}} v_L |v_L| + \frac{N_{rr}}{I_z - N_{\dot{r}}} r_L |r_L| + \frac{N_{ur}}{I_z - N_{\dot{r}}} u_L r_L + \frac{N_{uv}}{I_z - N_{\dot{r}}} u_L v_L + \frac{N_{uu\delta_r} {u_L}^2 \delta_{rL}}{I_z - N_{\dot{r}}} \tag{4.4}$$

The hydrodynamic parameters of the AUV are defined in Table 3.1. T_L and δ_{rL} are the thruster force and rudder orientation for the leader AUV. The control laws are developed as described in Section 3.6.

4.3.2 Follower AUV

This Section describes the kinematics and dynamics for the follower AUVs. As we assumed that the kinematics and dynamics for leader and follower AUV are the same, the kinematic equations of the followerAUVs can be represented as

$$\begin{aligned} \dot{x_F} &= u_F \cos(\psi_F) - v_F \sin(\psi_F) \\ \dot{y_F} &= u_F \sin(\psi_F) + v_F \cos(\psi_F) \\ \dot{\psi_F} &= r_F \end{aligned} \tag{4.5}$$

where to x_F, y_F are the positions and ψ_F is the angular position with reference to the Inertial frame I for the follower vehicles. u_F, v_F are the follower velocity along surge and sway motion and r_F is the angular motion along the yaw direction.
The dynamics considered for follower AUV is the same with that of the leader AUV but the coupling of rudder angle between sway and yaw motion is not considered in follower AUV for simplicity. So the dynamics of the follower AUV can be expressed as,

$$\dot{u_F} = \frac{m + X_{vr}}{m - X_{\dot{u}}} v_F r_F + \frac{X_{uu}}{m - X_{\dot{u}}} {u_F}^2 + \frac{T_F}{m - X_{\dot{u}}} \tag{4.6}$$

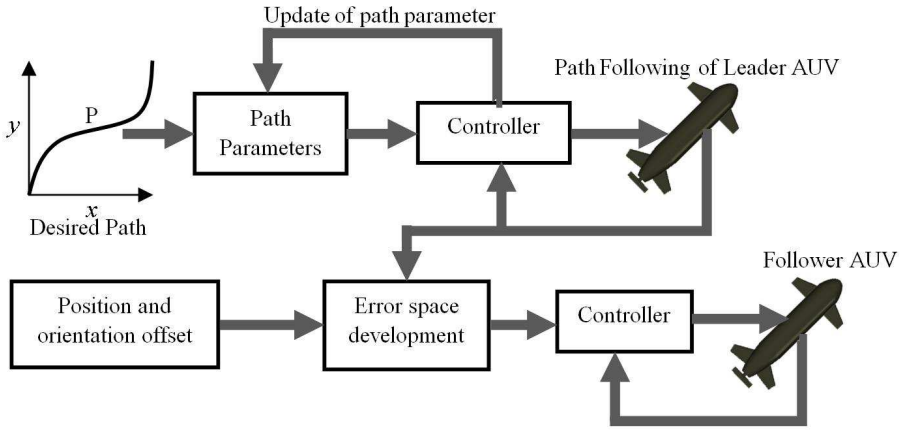

Figure 4.2: Control signal flow of error space for Leader-Follower

The equation of motion along sway direction is given by

$$\dot{v_F} = -\left(\frac{m - Y_{ur}}{m - Y_{\dot{v}}}\right) u_F r_F + \frac{Y_{uv}}{m - Y_{\dot{v}}} u_F v_F + \frac{Y_{vv}}{m - Y_{\dot{v}}} v_F \left|v_F\right| \tag{4.7}$$

The equation of motion along yaw direction is given by

$$\dot{r_F} = \frac{N_{vv}}{I_z - N_{\dot{r}}} v_F \left|v_F\right| + \frac{N_{rr}}{I_z - N_{\dot{r}}} r_F \left|r_F\right| + \frac{N_{ur}}{I_z - N_{\dot{r}}} u_F r_F + \frac{N_{uv}}{I_z - N_{\dot{r}}} u_F v_F + \frac{N_{uu\delta_r} {u_F}^2 \delta_{rL}}{I_z - N_{\dot{r}}} \tag{4.8}$$

where T_F and δ_{rF} are the thruster force and rudder orientation for the follower AUVs. These control inputs are obtained by designing the controller such that it enables the follower AUV to move in a desired formation structure.

4.4 Backstepping Strategy for Formation Control

4.4.1 Error Space Development

In this Section the error space between the leader AUV and the follower AUVs for the desired formation structure is developed considering the states of the leader AUV and the desired position and orientations as shown in Fig.4.2. For leader-follower formation it is required that the follower should maintain a desired distance at a particular angle. Hence, referring to Fig.4.3, a virtual frame is defined at the desired location of x_{FD} and y_{FD} which satisfies the desired distance d and desired angle θ_δ from the leader AUV.

The orientation of the virtual frame is considered as the same as that of leader AUV i.e. ψ_L. Let the initial position of follower AUV be x_F and y_F with an orientation of ψ_L. Then the error between the follower AUV and desired frame can be expressed with reference to the follower AUV as x_{EF} and y_{EF}.

The desired location for virtual frame is considered at a distance d and orientation θ_δ

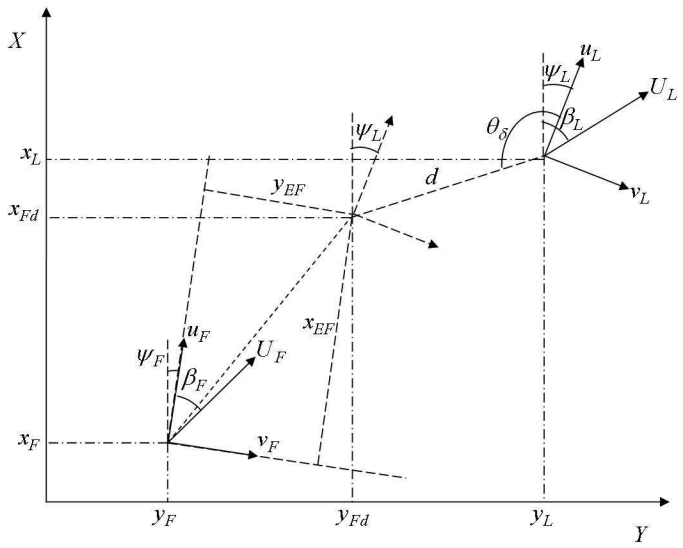

Figure 4.3: Development of Error space for Leader-Follower

from the leader AUV. Then the position of desired frame can be expressed as

$$\begin{aligned} x_{Fd} &= x_L + d\cos(\theta_\delta - \psi_L) \\ y_{Fd} &= y_L - d\sin(\theta_\delta - \psi_L) \end{aligned} \tag{4.9}$$

The difference between the desired frame and follower frame is considered as the error space. This error space enables the follower AUV to approach to the desired position and the error between follower frame and the desired frame is given by

$$\begin{bmatrix} x_{EF} \\ y_{EF} \end{bmatrix} = \begin{bmatrix} \cos\psi_F & \sin\psi_F \\ -\sin\psi_F & \cos\psi_F \end{bmatrix} \begin{bmatrix} x_{Fd} - x_F \\ y_{Fd} - y_F \end{bmatrix} \tag{4.10}$$

Taking the derivative of the above error equation and expressing in an expanded form one obtains

$$\begin{aligned} \dot{x}_{EF} = (\dot{x}_{Fd} - \dot{x}_F)\cos(\psi_F) - (x_{Fd} - x_F)\sin(\psi_F)\, r_F + (\dot{y}_{Fd} - \dot{y}_F)\sin(\psi_F) \\ + (y_{Fd} - y_F)\cos(\psi_F)\, r_F \end{aligned} \tag{4.11}$$

$$\begin{aligned} \dot{y}_{EF} = -(\dot{x}_{Fd} - \dot{x}_F)\sin(\psi_F) - (x_{Fd} - x_F)\cos(\psi_F)\, r_F + (\dot{y}_{Fd} - \dot{y}_F)\cos(\psi_F) \\ - (y_{Fd} - y_F)\sin(\psi_F)\, r_F \end{aligned} \tag{4.12}$$

By replacing the $\dot{x}_F$ and $\dot{y}_F$ from the kinematics equation of follower AUV described in (4.5), then the equation.4.11 can be expressed as

$$\begin{aligned} \dot{x}_{EF} &= u_L\cos(\psi_L - \psi_F) - v_L\sin(\psi_L - \psi_F) + r_L d\sin(\theta_\delta - \psi_L + \psi_F) + r_F y_{EF} - u_F \\ \dot{y}_{EF} &= u_L\sin(\psi_L - \psi_F) + v_L\cos(\psi_L - \psi_F) + r_L d\cos(\theta_\delta - \psi_L + \psi_F) - r_F x_{EF} - v_F \end{aligned} \tag{4.13}$$

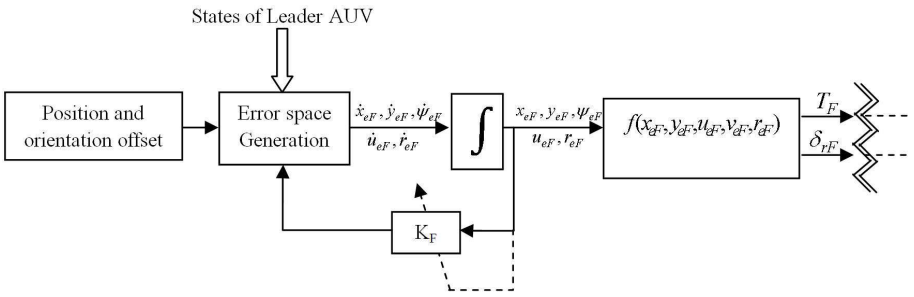

Figure 4.4: The proposed structure of formation controller for follower AUVs

and by substituting $u_L = U_L \cos\beta_L$ and $v_L = U_L \sin\beta_L$ in the above equation then can be expressed in a more compact form. Hence the final expression for error space between leader and follower AUV can be represented as follows

$$\begin{aligned} \dot{x}_{EF} =& U_L \cos\left(\psi^*_{EF}\right) + r_L d \sin\left(\theta_\delta - \psi_L + \psi_F\right) + r_F y_{EF} - u_F \\ \dot{y}_{EF} =& U_L \sin\left(\psi^*_{EF}\right) + r_L d \cos\left(\theta_\delta - \psi_L + \psi_F\right) - r_F x_{EF} - v_F \end{aligned} \tag{4.14}$$

where $\psi^*_{EF} = \beta_L + \psi_L - \psi_F$, the above error equation represents the error space with reference to x and y axis and ψ^*_{EF} represents the orientation difference between leader AUV and follower AUV.

4.4.2 Control Law Development

For developing the control law for follower AUV, the Lyapunov functions are defined which are functions of error space developed in the Section 4.4.1. By solving these Lyapunov functions and considering the positive constant gains, it can be shown that the close loop is stable.

Initially it is assumed that $\psi^*_{EF} = \alpha_{\psi^*_{EF}}$, where $\alpha_{\psi^*_{EF}}$ is the angle that describes the desired orientation for follower AUV to follow the leader AUV.A Lyapunov function V_{1F} is considered for minimizing the error between virtual frame and actual body frame of follower AUV. Let the Lyapunov function is defined as

$$V_{1F} = \frac{1}{2}\left(x^2_{EF} + y^2_{EF}\right) \tag{4.15}$$

In order for the closed loop system to be stable the derivative of the Lyapunov function should always be negative. Hence, taking the derivative of the V_{1F} leads to

$$\dot{V}_{1F} = x_{EF}\dot{x}_{EF} + y_{EF}\dot{y}_{EF} \tag{4.16}$$

and replacing $\dot{x}_{EF}$ and $\dot{y}_{EF}$ in (4.17) from (4.14), the expression of $\dot{V}_{1F}$ can be represented as

$$\begin{aligned} \dot{V}_{1F} = & U \cos\left(\psi_L - \psi_F + \beta\right) x_{EF} + r_L d \sin\left(\theta_\delta - \psi_L - \psi_F\right) x_{EF} - u_F x_{EF} \\ & + U \sin\left(\psi_L - \psi_F + \beta\right) y_{EF} + r_L d \cos\left(\theta_\delta - \psi_L - \psi_F\right) y_{EF} - v_F y_{EF} \end{aligned} \tag{4.17}$$

Assuming that $\psi_L - \psi_F + \beta = \alpha_F$, where α_F is the desired orientation of follower AUV and rewriting the above equation by taking x_{EF} and y_{EF} as common variables as follows

$$\begin{aligned}\dot{V}_{1F} = &\left(U\cos\left(\alpha_F\right) + r_L d\sin\left(\theta_\delta - \psi_L - \psi_F\right) - u_F\right) x_{EF} \\ &+ \left(U\sin\left(\alpha_F\right) + r_L d\cos\left(\theta_\delta - \psi_L - \psi_F\right) - v_F\right) y_{EF} \end{aligned} \quad (4.18)$$

From (4.18) if u_F is selected as follows

$$u_F = K_{x_{EF}}\tanh\left(x_{EF}\right) + U_L\cos\left(\psi_L - \psi_F + \beta_L\right) + r_L d\sin\left(\theta_\delta - \psi_L - \psi_F\right) \quad (4.19)$$

then (4.18) can be represented as

$$\dot{V}_{1F} \;=\; -x_{EF}K_{x_{EF}}\tanh\left(x_{EF}\right) \;+\; y_{EF}U\sin\left(\alpha_F\right) \;+\; y_{EF}\left(r_L d\cos\left(\theta_\delta - \psi_L - \psi_F\right) - v_F\right) \quad (4.20)$$

The term $y_{EF}U\sin\left(\alpha_F\right)$ is always be negative if the desired orientation α_F is chosen as

$$\alpha_F = -\theta_a\tanh\left(K_{\delta_F}y_{EF}\right) \quad (4.21)$$

Thus, in chapter 3 the stability of the leader motion is shown as stable, so it can be concluded that $r_L d\cos\left(\theta_\delta - \psi_L - \psi_F\right) < \epsilon$ as r_L has a definite value and ϵ has a definite value. Later of the stability proof it is shown that v_F is also bounded. As y_{EF} has a finite range then the total Lyapunov function is always a bounded function.
Let the deviation of actual angular position from the the desired angular is defined by $\bar{\psi}_{EF} = \psi^*_{EF} - \alpha_{\psi^*_{EF}}$. Then its derivative can be expressed as,

$$\begin{aligned}\dot{\bar{\psi}}_{EF} =&\dot{\psi}_L - \dot{\psi}_F + \frac{u_L\dot{v}_L - v_L\dot{u}_L}{U_L} - \dot{\alpha}_F \\ =&r_L - r_F + \frac{u_L\dot{v}_L - v_L\dot{u}_L}{U_L} - \dot{\alpha}_F\end{aligned} \quad (4.22)$$

Introducing the term α_{rF} which represents the desired angular velocity for the follower AUV. Then defining a Lyapunov candidate function V_{2F}, which is a function of $\bar{\psi}_{EF}$. Defining a Lyapunov function V_{2F} which is a positive definite function of $\bar{\psi}_{eF}$. Let the defined Lyapunov function is given as follows,

$$V_{2F} = \frac{1}{2}\bar{\psi}^2_{EF} \quad (4.23)$$

then differentiating it with respect to time and replacing $\dot{\bar{\psi}}_{EF}$ from (4.22), the $\dot{V}_{2F}$ can be represented as

$$\begin{aligned}\dot{V}_{2F} =&\bar{\psi}_{EF}\dot{\bar{\psi}}_{EF} \\ =&\bar{\psi}_{EF}\left(r_L - r_F + \frac{u_L\dot{v}_L - v_L\dot{u}_L}{U_L} - \dot{\alpha}_F\right)\end{aligned} \quad (4.24)$$

in the above equation $r_F = r_{eF} + \alpha_{rF}$ and α_{rF} is the desired yaw velocity. Applying backstepping approach and choosing α_{rF} as the control input then by assigning

$$\alpha_{rF} = r_L + \frac{u_L \dot{v}_L - v_L \dot{u}_L}{U_L} - \dot{\alpha}_F + K_{\psi_{EF}} \bar{\psi}_{EF} \tag{4.25}$$

the (4.24) can be expressed as

$$\dot{V}_{2F} = -r_{EF} \bar{\psi}_{EF} - K_{\psi_{EF}} \bar{\psi}_{EF}^2 \tag{4.26}$$

From the expression of $\dot{V}_{2F}$, it is clear that if r_{EF} reduces to zero, then the error function V_{2F} reduces to zero. Referring to (4.19), the desired surge velocity is developed and it is required that the actual surge velocity should approach to the desired velocity. To avoid confusion in parameter notations, the u_F of (4.19) is replaced as u_{Fd}. The u_{Fd} for the follower AUV is represented as following

$$u_{Fd} = K_{x_{EF}} \tanh(x_{EF}) + U_L \cos(\psi_L - \psi_F + \beta_L) + r_L d \sin(\theta_\delta - \psi_L - \psi_F) \tag{4.27}$$

The deviation of actual surge velocity from desired surge velocity is represented as,

$$u_{eF} = u_F - u_{Fd} \tag{4.28}$$

and taking its derivative and replacing r_F with $r_{eF} + \alpha_{rF}$ results the following equation.

$$\dot{u}_{eF} = \left(\frac{m + X_{vr}}{m - \dot{X}_u}\right) v_F r_{eF} + \left(\frac{m + X_{vr}}{m - \dot{X}_u}\right) v_F \alpha_{rF} + \left(\frac{X_{uu}}{m - \dot{X}_u} {u_F}^2\right) + \left(\frac{T_{u_F}}{m - \dot{X}_u}\right) - \dot{u}_{FD} \tag{4.29}$$

A Lyapunov function V_{3F} is considered for reducing the error of surge velocity, the Lyapunov function is defined as

$$V_{3F} = \frac{1}{2} {u_{eF}}^2 \tag{4.30}$$

where $u_{eF} = u_F - u_{Fd}$ is the difference between actual surge velocity and desired surge velocity. Taking the derivative of the Lyapunov function V_{3F} and replacing it with required $\dot{u}_{eF}$ from (4.29), then the $\dot{V}_{3F}$ is given by

$$\dot{V}_{3F} = u_{eF} \left(\frac{m + X_{vr}}{m - \dot{X}_u}\right) v_F r_{eF} + \left(\frac{m + X_{vr}}{m - \dot{X}_u}\right) v_F \alpha_{rF} + \left(\frac{X_{uu}}{m - \dot{X}_u} {u_F}^2\right) + \left(\frac{T_{u_F}}{m - \dot{X}_u}\right) - \dot{u}_{FD} \tag{4.31}$$

As the expression includes thruster force as control input. So if this control input T_{uF} is selected as follows

$$T_{u_F} = \left(-K_{u_{EF}} u_{EF} + \dot{u}_{FD}\right) \left(m - \dot{X}_u\right) - X_{uu} {u_F}^2 - \left(m + X_{vr}\right) v_F \alpha_{rF} \tag{4.32}$$

then the derivative of the Lyapunov function V_{3F} can be represented as following,

$$\dot{V}_{3F} = \left(\frac{m + X_{vr}}{m - X_{\dot{u}}}\right) v_F r_{eF} u_{eF} - K_{u_{EF}} {u_{EF}}^2 \tag{4.33}$$

It is clear from (4.33) that if $v_F r_{EF}$ is proved to be a bounded or decreasing function then the actual surge velocity of follower AUV will approach to the desired surge velocity. Gain K_{u_F} is considered as a positive gain. Analyzing (4.26) and (4.33), it is clear that if the error in yaw angular velocity decreases then the follower AUV is globally stable and approaches to the virtual frame exponentially.

Recalling the expression for yaw error velocity $r_{EF} = r_F - \alpha_{rF}$, taking its derivative and with replacing with $\dot{r}_F$ from (4.8), $\dot{r}_{EF}$ can be expressed as

$$\dot{r}_{EF} = \frac{N_{vv}}{I_z - N_{\dot{r}}} v_F |v_F| + \frac{N_{rr}}{I_z - N_{\dot{r}}} r_F |r_F| + \frac{N_{ur}}{I_z - N_{\dot{r}}} u_F r_F + \frac{N_{uv}}{I_z - N_{\dot{r}}} u_F v_F + \frac{N_{uu\delta_r} {u_F}^2 \delta_{rL}}{I_z - N_{\dot{r}}} - \dot{\alpha}_{rF} \tag{4.34}$$

Defining a Lyapunov function V_{4F}, which is a positive definite function of the yaw velocity error r_{EF} as follows

$$V_{4F} = \frac{1}{2} {r_{eF}}^2 + V_{2F} + V_{3F} \tag{4.35}$$

Taking the derivative of the Lyapunov function and replacing $\dot{V}_{2F}$ and $\dot{V}_{3F}$ from (4.26) and (4.33) is represented as follows

$$\dot{V}_{4F} = r_{eF}\dot{r}_{eF} - r_{EF}\bar{\psi}_{EF} - K_{\psi_{EF}}\bar{\psi}_{EF}^2 + \left(\frac{m + X_{vr}}{m - X_{\dot{u}}}\right) v_F r_{eF} u_{eF} - K_{u_{EF}} {u_{EF}}^2 \tag{4.36}$$

From the above Lyapunov function replacing $\dot{r}_{eF}$ from (4.34) and considering the rudder orientation as

$$\begin{aligned} \delta_{rF} = \left(\frac{N_{uu\delta_r}}{I_z - N_{\dot{r}}} {u_F}^2\right)^{-1} \Bigg(& -K_{r_{eF}} r_{eF} - \frac{m + X_{vr}}{m - X_{\dot{u}}} v_F u_{eF} + \bar{\psi}_{eF} - \frac{N_{uv}}{I_z - N_{\dot{r}}} u_F v_F \\ & - \frac{N_{vv}}{I_z - N_{\dot{r}}} |v_F| v_F + \dot{\alpha}_{rF} - \left(\frac{N_{rr}}{I_z - N_{\dot{r}}} |r_F| + \frac{N_{ur}}{I_z - N_{\dot{r}}} u_F\right) \alpha_{rF} \Bigg) \end{aligned} \tag{4.37}$$

then the derivative of the Lyapunov function V_{4F} can be considered as follows,

$$\dot{V}_{4F} = -K_{\psi_{eF}} \bar{\psi}_{eF}^2 - K_{u_{eF}} {u_{eF}}^2 - K_{r_{eF}} {r_{eF}}^2 + \left(\frac{N_{rr}}{I_z - N_{\dot{r}}} |r_F| + \frac{N_{ur}}{I_z - N_{\dot{r}}} u_F\right) r_{eF} \tag{4.38}$$

In the above expression of $\dot{V}_{4F}$, $K_{r_{eF}}$ are positive gains and referring to the hydrodynamic parameters of AUV it is clear that $\left(\frac{N_{rr}}{I_z - N_{\dot{r}}} |r_F| + \frac{N_{ur}}{I_z - N_{\dot{r}}} u_F\right)$ is always a negative quantity. So it is proved that by choosing the control law given in (4.32) and (4.37) for thruster force and rudder angle respectively.An optimization approach can be implemented [48] for adjusting the gain of the followers for better formation control.

4.5 Fuzzy Controller for Formation Control

Since the dynamics of an AUV is uncertain and the formation control of multiple AUVs involve several uncertainties. Further a fuzzy logic controller is employed in this section

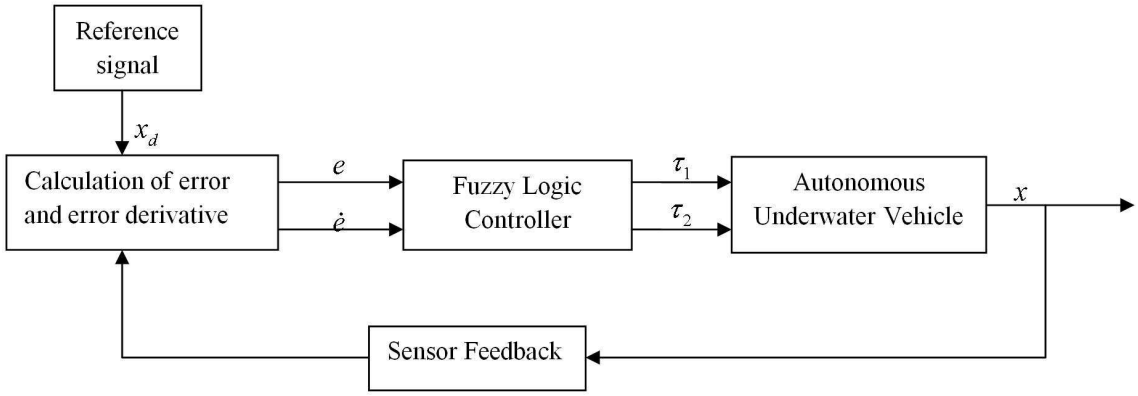

Figure 4.5: Block diagram of the AUV with fuzzy controller

for achieving formation control. The overview structure of the closed loop of the plant and controller is shown in Fig.4.5. As shown in the figure the error block calculates the error and error derivative between the current state of the AUV and desired signal. Fuzzy logic controller accepts these errors and generates the suitable control input which enables the AUV to successfully track the desired path. The Fuzzy Logic Controller is derived considering the AUV kinematics and it is assumed that there exists another controller which stabilizes the inner loop.

4.5.1 Design of Fuzzy Logic Controller

For developing the fuzzy logic controller(FLC) the error inputs considered are x_{EF} and y_{EF}, these errors are the distance between the follower AUV and the desired virtual frame as shown in Fig.4.3. Considering the plant as AUV kinematics as in (4.5) the fuzzy logic controller is designed to generate the suitable control input u_F and r_F which will drive the follower to the virtual frame. From the Fig.4.3, x_{EF} and y_{EF} is used to design the FLC for the u_F control input. FLC for r_F control input is designed using the angular error θ_E and $\dot{\theta}_E$, where θ_E can be defined as

$$\theta_E = -\theta_A \tanh\left(K y_{EF}\right) \tag{4.39}$$

Linguistic Variables

There are six i/o parameter used to develop the FLC, the linguistic used to describe the states of these parameters are defined in Table.4.1.

Membership Function

For defining the fuzzy variables the trapezoidal membership functions are chosen. For input and output variables the states are represented as linguistic variables and each variable is associated with trapezoidal membership function.

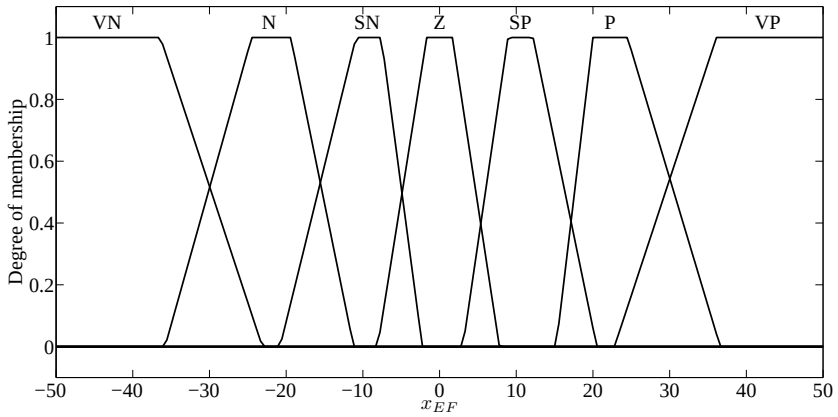

Figure 4.6: Fuzzy Membership function for error along x-axis

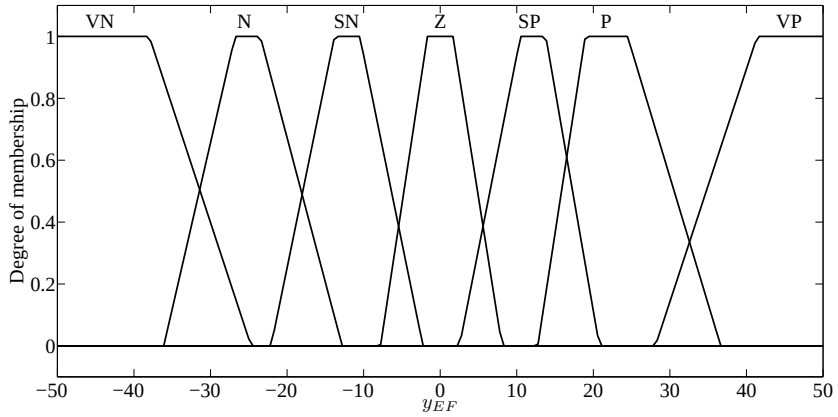

Figure 4.7: Fuzzy Membership function for error along y-axis

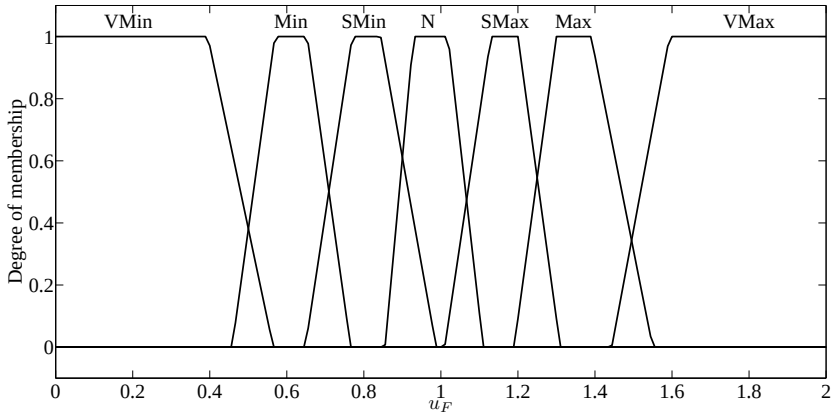

Figure 4.8: Fuzzy membership function for surge velocity

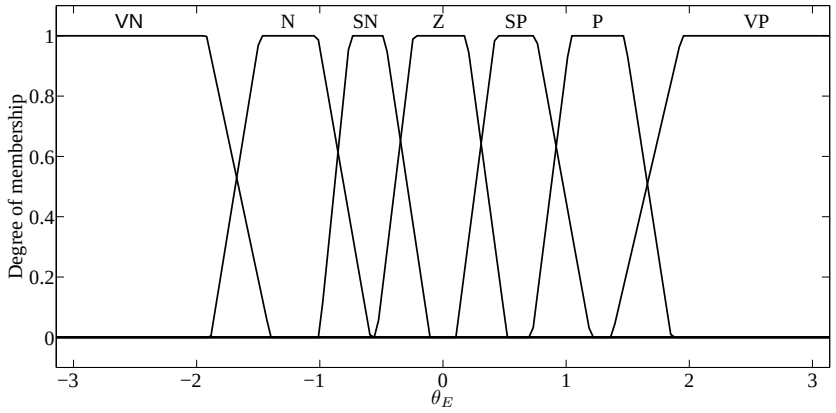

Figure 4.9: Fuzzy membership function of angular error

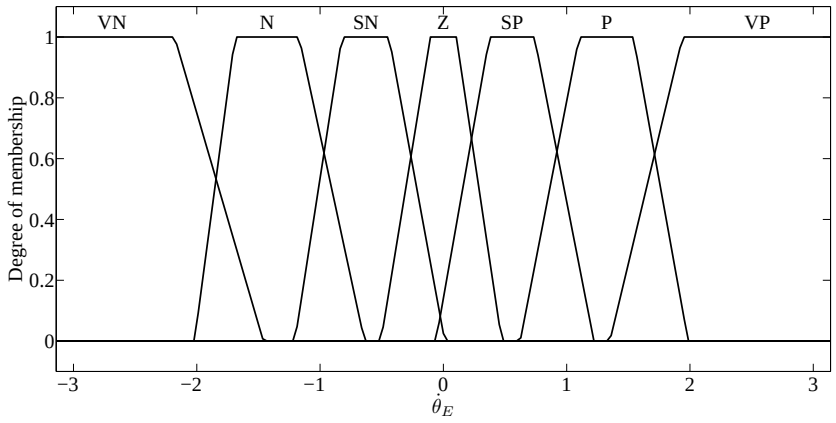

Figure 4.10: Fuzzy membership function for derivative of angular error

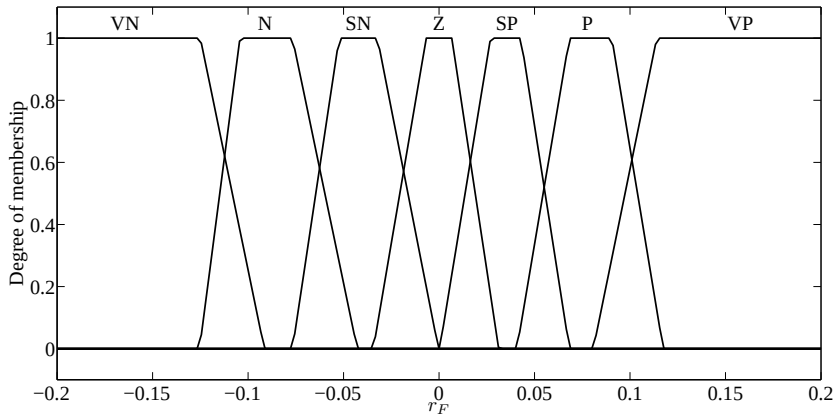

Figure 4.11: Fuzzy membership function for yaw velocity

VN	Very Negative
N	Negative
NS	Negative Small
Z	Zero
PS	Positive Small
P	Positive
VP	Very Positive
VMIN	Very Minimum
MIN	Minimum
SMIN	Small Minimum
N	Normal
SMAX	Small Maximum
MAX	Maximum
VMAX	Very Maximum

Table 4.1: Linguistic variables for input and output parameters

y_{EF} \ x_{EF}	VN	N	SN	Z	SP	P	VP
VN	VMin	VMin	VMin	VMin	Min	SMin	N
N	VMin	VMin	VMin	Min	SMin	N	SMax
SN	VMin	VMin	Min	SMin	N	SMax	Max
Z	VMin	Min	SMin	N	SMax	Max	VMax
SP	VMin	VMin	Min	SMin	N	SMax	Max
P	VMin	VMin	VMin	Min	SMin	N	SMax
VP	VMin	VMin	VMin	VMin	Min	SMin	N

Table 4.2: Fuzzy rule base for forward motion control

For developing the controller for follower AUVs two rule base is designed as it has two control inputs. These rule base are the knowledge base and these are implemented using IF - THEN rules. A proper rule base is to be designed which will force the follower AUV to steer towards the desired frame. The rule base table explains the relationship between input and output fuzzy variables defined as membership function. Table.4.2 is designed for the control of surge motion of the AUV. The rule base can be designed by analyzing the behavior of the AUV under control. For designing the rule base for forward motion it is considered that if x_{EF} is positive which means follower is behind the leader then the surge velocity(u_F) should increase. Similarly if x_{EF} is negative i.e. follower is ahead of leader then the desired surge velocity (u_F) should be a fixed nominal value. The y_{EF} input controls the magnitude of the surge velocity of the AUV. If y_{EF} is more than the magnitude of the surge velocity will decrease irrespective of x_{EF}. Table.4.3 is designed for the control of angular motion of the AUV i.e. yaw motion. Initially the

$\dot{\theta}_E$ \ θ_E	VN	N	SN	Z	SP	P	VP
VN	VP	VP	VP	VP	P	SP	Z
N	VP	VP	VP	P	SP	Z	SN
SN	VP	VP	P	SP	Z	SN	N
Z	VP	P	SP	Z	SN	N	VN
SP	P	SP	Z	SN	N	VN	VN
P	SP	Z	SN	N	VN	VN	VN
VP	Z	SN	N	VN	VN	VN	VN

Table 4.3: Fuzzy rule base for angular motion control

angular error(θ_E) and derivative of the angular error($\dot{\theta}_E$) are derived using x_{EF} and y_{EF} as in (4.39). Considering the error and change of error a fuzzy rule base is designed which imitates the properties of PD control. For example if θ_E is Positive Small(SP) and $\dot{\theta}_E$ is Negative Small(NS) then control output r_F will be Zero(Z).

Defuzzification

After implementing the fuzzy inference system the output will be a fuzzy and it should be transformed to crisp value for supplying to the plant. The method of conversion of fuzzy variable to crisp variable is called defuzzification. There are different defuzzification techniques are available such as centroid, bisector, Middle of Maximum(MOM), Smallest of Maximum(SOM) and Largest of Maximum(LOM). Out of this for our system the centroid method is adopted because of its simplicity. The following is the expression for centroid method technique,

$$x_t = \frac{\int \mu_i(x)\, x dx}{\int \mu_i(x)\, dx} \tag{4.40}$$

where x_t is the net output of the defuzzifier, x is the fuzzy output and μ_i represents the aggregate membership function.

4.6 Results and Discussions

The formation control law derived in the Section 4.4.2 was simulated using MATLAB and the control law for the leader AUV control law which was derived for the single AUV in the chapter 3. The desired shape for the formation control is chosen as a triangular shape as shown in Fig.4.12. It is assumed that the dynamics of the follower AUVs is same as that of the leader AUV.

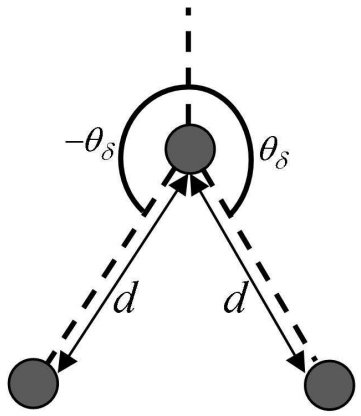

Figure 4.12: Desired formation shape for formation control

Table 4.4: Comparison of backstepping and fuzzy logic control algorithms

Comparison	Surge velocity(u_f)	Yaw velocity(r_f)	Velocity profile
Backstepping Controller	$u_f \leq 1.1$	$-0.15 \leq r_f \leq 0.2$	smooth
Fuzzy Logic Controller	$u_f \leq 1.3$	$-0.032 \leq r_f \leq 0.068$	switching

Fig.4.13 shows the effectiveness of the backstepping controller for the formation of three AUVs in a triangular shape. While traversing the desired path the error corresponding to the leader AUV position and the desired path is shown in Fig.4.14. The error for follower AUVs to maintain the desired triangular shape are shown in Fig.4.15 and Fig.4.16.The desired surge velocity for the leader AUV is provided as $1m/sec$ as shown in Fig.4.17 for traversing the circular path. Intuitively it can be said the velocity of follower AUV which is inside the circular path should have lower surge velocity than the leader AUV. Whereas the follower AUV which is at the outer of the circular path should have higher velocity than the leader AUV. This is observed in Fig.4.17. The yaw orientation of the three AUV's are shown in Fig.4.18. Whereas, Fig.4.19 represents the angular yaw velocity of the leader AUV and Fig.4.20 are the angular yaw velocities for the respective follower AUVs. The results of the fuzzy logic controller which is derived in Section 4.5.1 are presented here, Fig.4.21 shows the formation control of the leader-follower. The control inputs which are required to drive the follower AUV kinematics towards the leader AUV are surge velocity(u_f) and yaw velocity(r_f). These generated control inputs are represented in Fig.4.22 and Fig.4.23 respectively. Table 4.4 shows the comparison between backstepping and fuzzy logic controller.

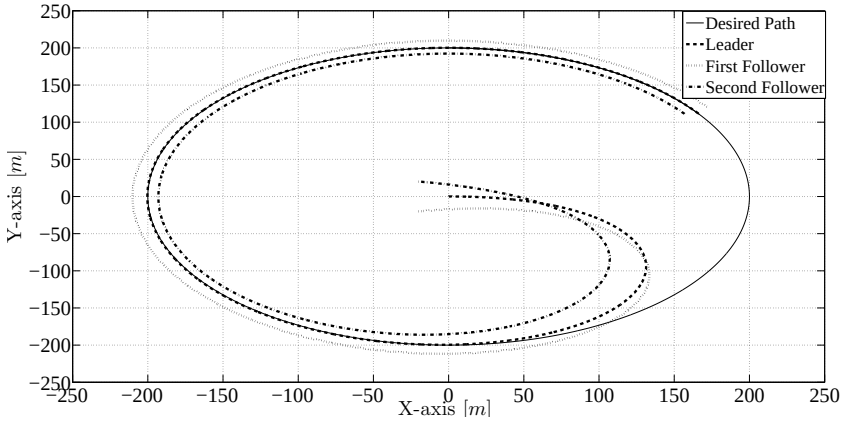

Figure 4.13: Formation of three AUV's maintaining a triangular shape

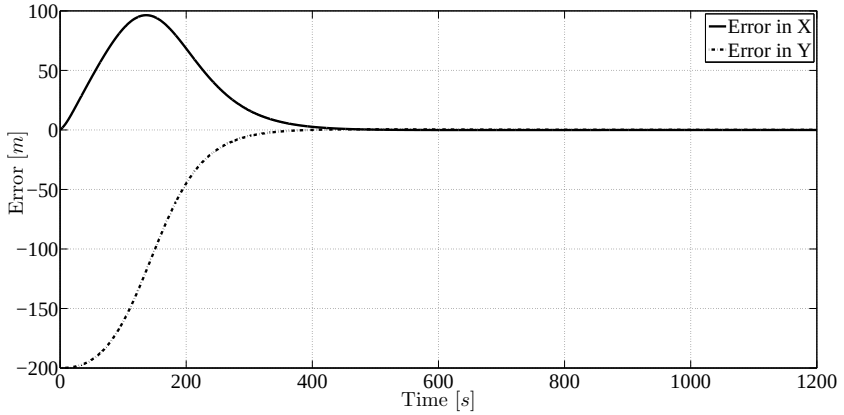

Figure 4.14: Error of the Leader AUV while traversing the desired path

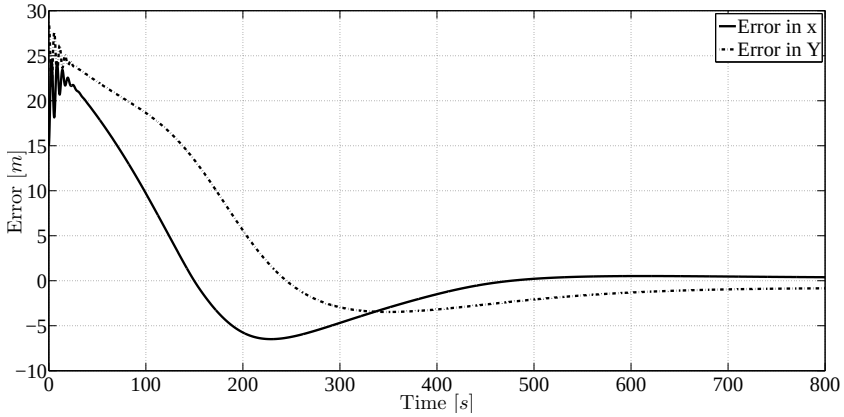

Figure 4.15: Error of follower AUV1 while following the Leader AUV

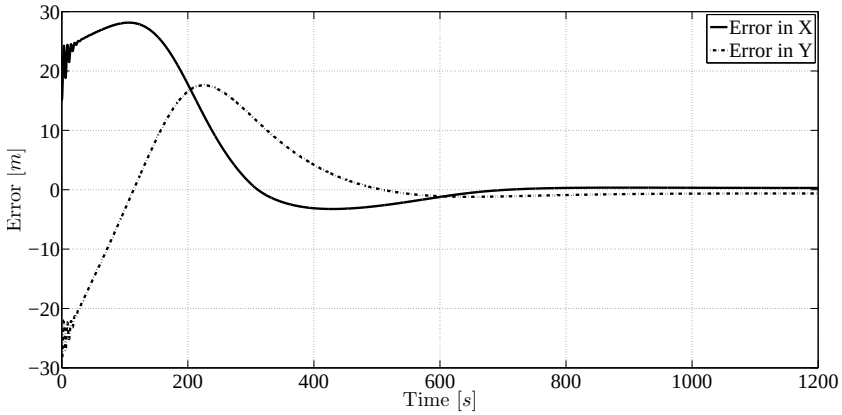

Figure 4.16: Error of follower AUV2 while following the Leader AUV

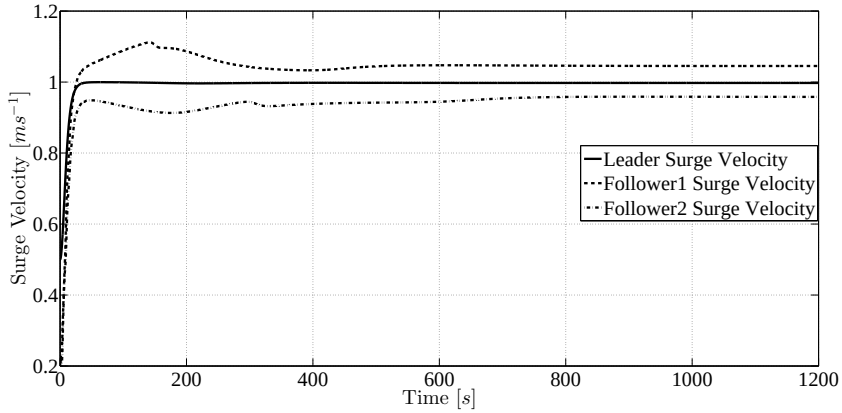

Figure 4.17: Surge velocity of three AUV's while following the desired path

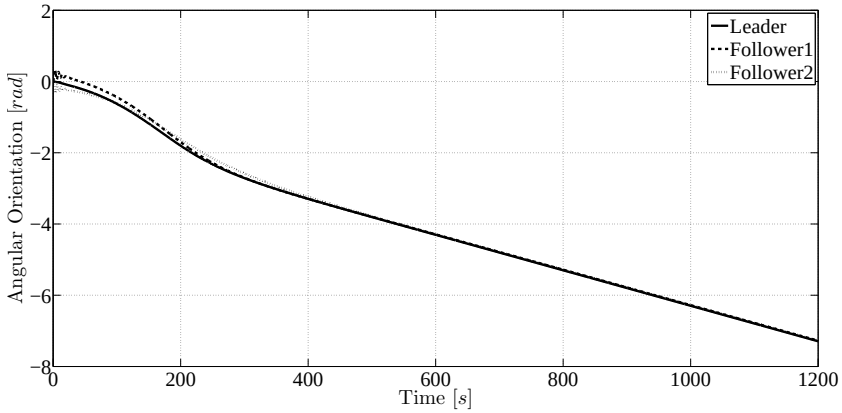

Figure 4.18: Angular orientation of three AUV's while following the desired path

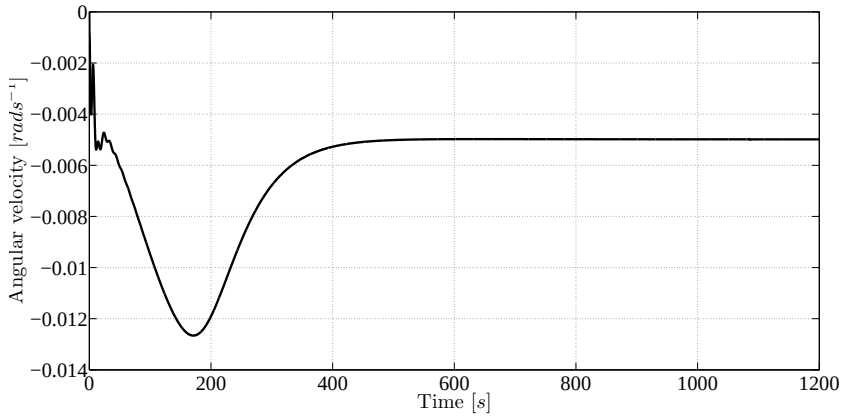

Figure 4.19: Angular velocity of Leader AUV variation w.r.t time

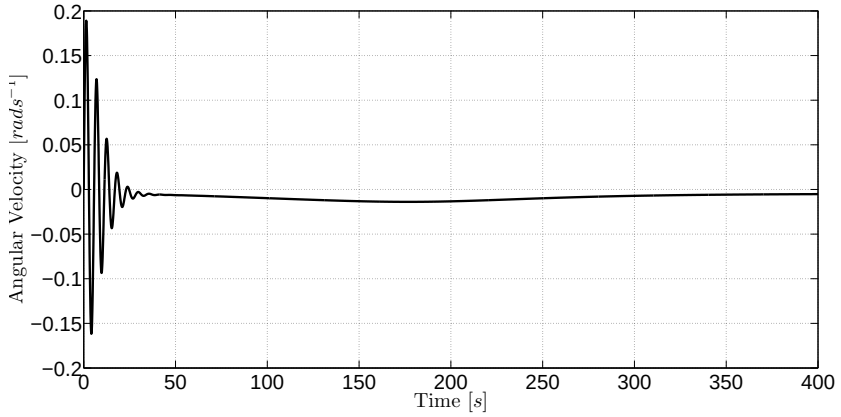

Figure 4.20: Angular velocity of Follower AUV1 variation w.r.t time

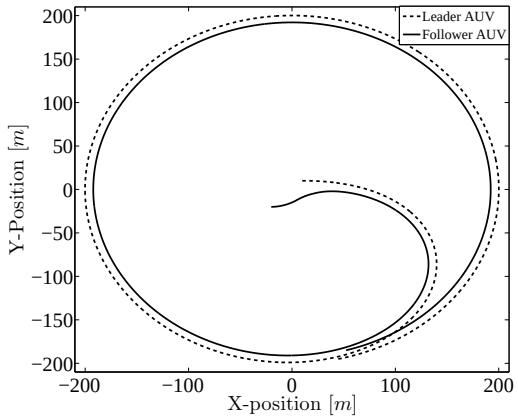

Figure 4.21: Formation control using fuzzy logic controller

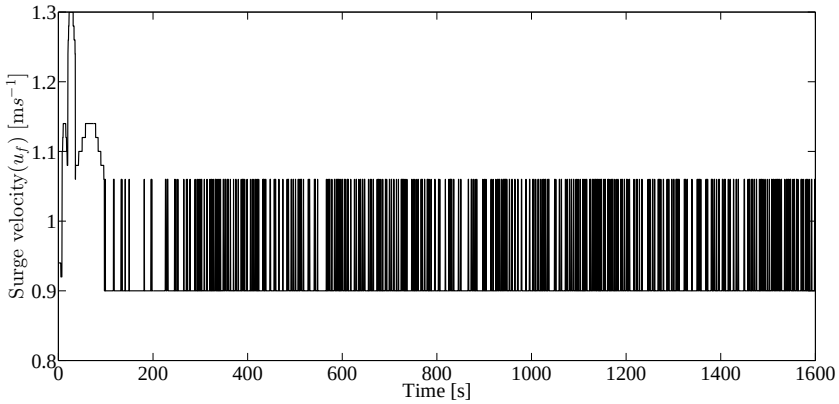

Figure 4.22: Control input for surge motion using fuzzy logic controller

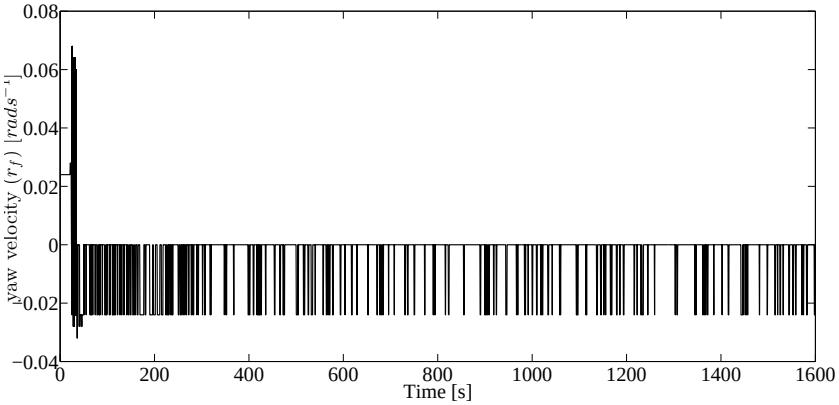

Figure 4.23: Control input for yaw motion using fuzzy logic controller

4.7 Chapter Summary

In this chapter a formation control law using the concept of Lyapunov based backstepping control law has been developed for maintaining a desired shape. It is also shown that by using Lyapunov criteria the follower AUV parameters such as linear and angular position and velocities remains in stable region while following the leader. Fuzzy logic controller has also been employed for leader-follower formation control problem. FLC enables to generate the desired surge and yaw velocity for the internal controller. In order to verify the efficiency of the proposed control law, a triangular shape is considered as desired formation shape and extensive simulations were pursued and results are analyzed. A comparison is also made between the proposed controllers and it is found from the results presented in section 4.6 that the backstepping controller performs better than the FLC in terms of control input for surge and yaw velocity.

Chapter 5

Graphical Visualization and Hardware Development of an AUV

5.1 Introduction

The lack of graphical visualization toolbox for Autonomous Underwater Vehicle(AUV) discourages many researchers and industries to work on AUV without having the physical prototype. These graphical visualization tool helps researchers, industries and end users to seamlessly interact with each other. Along with the control system, graphical visualization is also very important because it enables us to visualize the motion of AUV.

This chapter is organized as follows. The development of a graphical visualization tool is described in Section 5.3. This sections describes the interaction of AUV model and environment model to successfully develop a graphical visualization toolbox. Results of graphical simulation of multiple AUVs at different time instant are discussed in Section 5.4. In the later part of this chapter, in Section 5.5, the hardware development of an AUV is proposed. In this Section the sensors, actuators and other electronics components are also discussed which are used for developing the AUV hardware.

5.2 Objective

This chapter deals with the development of a graphical tool, which will be used for visualizing the motion of a single AUV as well as motion of multiple AUVs in an ocean environment. Graphical visualization tool is used to analyze the result of Chapter 3 and Chapter 4. Along with the development of graphical tool, this chapter also discusses about the hardware implementation of an AUV. This chapter describes the following two objectives.

- Development of a graphical user interface and graphical visualization for visualizing the motion of AUV or multiple AUVs

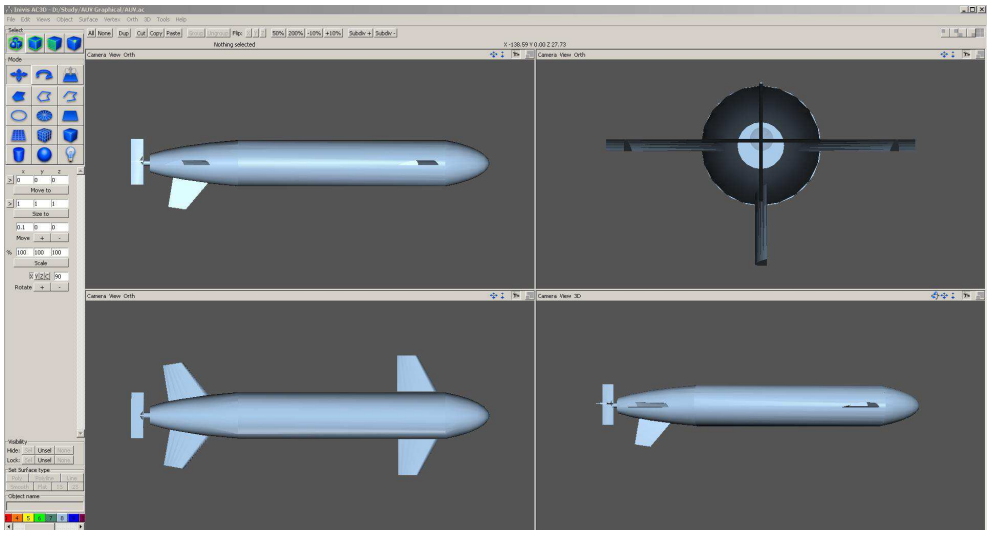

Figure 5.1: Design of AUV model

- Hardware Realization of an AUV.

5.3 Development of Graphical Visualization Tool

Virtual Reality Modeling Language(VRML) is used for the developing the graphical environment. Graphical software such as AC3D and Blender3D are used for developing the AUV model and ocean environment. AC3D is a graphical design software developed in 1994, this software is mostly used for developing the 3D environment for simulation purpose. The major advantage of using this software is that it supports to numerous graphical formats and also exports many graphical formats. Another software which can be used in the context of graphical environment or AUV model design in Blender3D. Both these software export VRML format which can be used by SIMULINK3D in MATLAB Toolbox for simulation.

5.3.1 Graphical model of an AUV

The AUV model is designed using AC3D as shown in Fig.5.1. The graphical models consist of surfaces and vertices to represent the solid surface. The number of these surfaces and vertices decides the smoothness and precision of the 3D model. So greater is the number of vertices and surface, better is the model quality but also the size of the 3D model gradually increases which again require high performance CPU for execution. Therefore, there is a tradeoff between the selection of number of graphical polygons. For our AUV model the number of surfaces and vertices 1344 and 1437 and total number of objects are 309. Fig.5.1 shows the development of AUV model and different orientations. For oceanic environment, the sea floor of Marine Visualization Toolbox is considered. Until now the

AUV model and sea floor have been developed and it is required that those models are to be combined so that a complete underwater environment along with AUVs can be represented which is described in the following section.

5.3.2 VRML of AUV

A VRML editor V-Realm Builder is used for developing the graphical scene comprising of ocean floor and AUV model designed using AC3D. V-Realm Builder is a tool for developing 3D objects and environment, which can be viewed using its own browser or with any other browser supporting VRML 2.0. The 3D model developed using V-Realm Builder as shown in Fig.5.2 are of less size, which enables us to create complex objects and successfully executes in a standard PC.

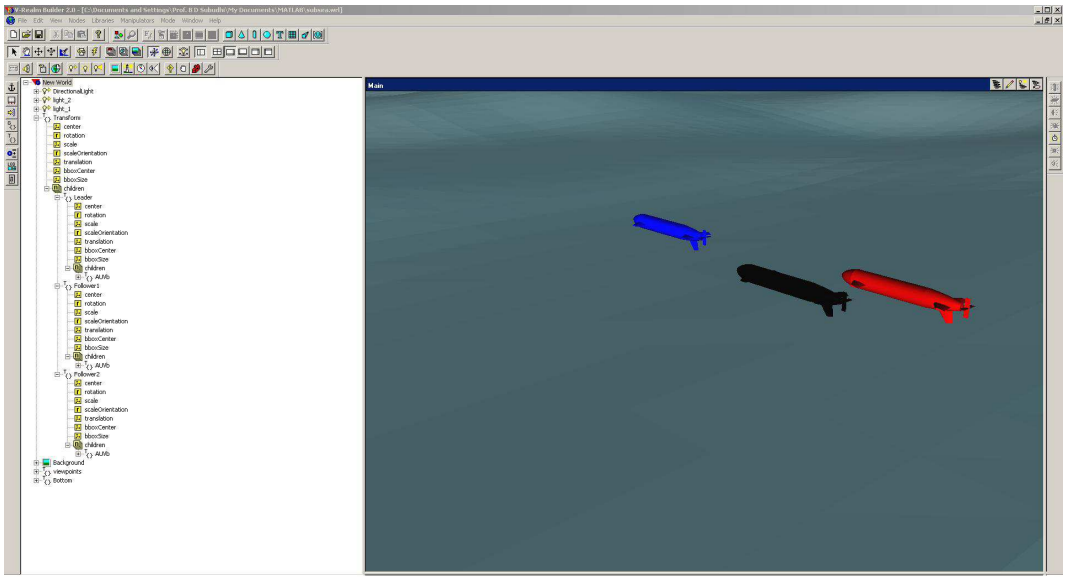

Figure 5.2: VRML of AUV

Control of Nodes

VRML models can be easily interfaced with SIMULINK3D and the control input generated from the controller can be directly applied to the AUV model inside the graphical environment. Fig.5.3 shows the nodes of the leader AUV, these nodes represent the links between SIMULINK and graphical interface. There are nodes which control the object center, object size and scale but for motion control objective the translation and rotational nodes are interfaced. The inputs generated by the control algorithm are supplied to the graphical environment through these nodes as shown in Fig.5.3 and the motion can be observed in the graphical window.

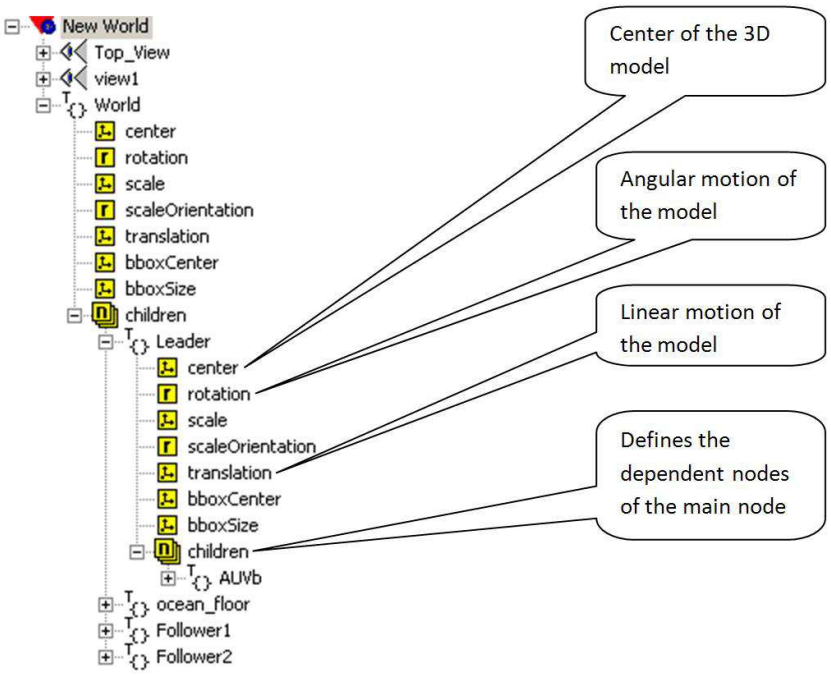

Figure 5.3: Control nodes of Leader AUV

5.4 Graphical Simulation : observations

The control law algorithm developed in Chapter 3 and Chapter 4 are simulated in the graphical environment and the results are shown in Fig.5.4 with different camera positions. The leader AUV tracks the desired path and the follower AUVs follows the leader thereby creates a formation structure.

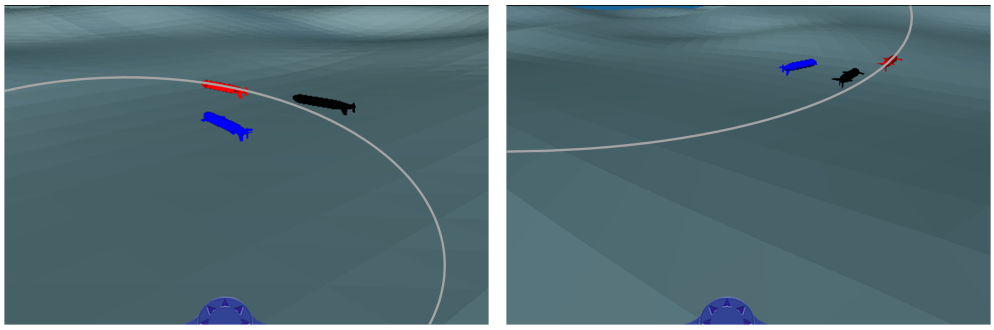

(a) Camera Position 1 (b) Camera Position 2

Figure 5.4: Graphical Visualization of Multiple AUVs

5.5 AUV Hardware Design

5.5.1 Mechanical Design

Structure Development: The vehicle shape has been fabricated using aluminium material. The interior sections of the AUV are covered with PVC foam or syntactic foam. These

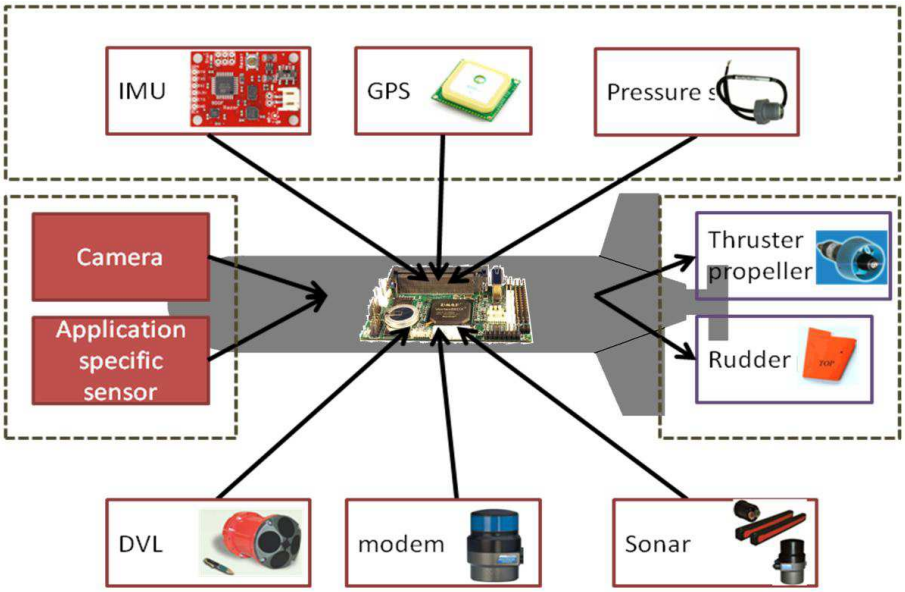

Figure 5.5: AUV sensors and control planes

foams are suitable for buoyancy adjustment and also due to the presence of micro balloons these materials are transparent to the sonar signal. The desired shape of the AUV is chosen as torpedo shape for low drag. [49] proposes the design of torpedo shaped AUVs for which the theoretical drag coefficient can be estimated. In accordance with [49], the shape of nose is expressed as follows

$$r = \frac{d}{2}\left\{1 - \left(\frac{x-a}{a}\right)\right\}^{\frac{1}{n}} \tag{5.1}$$

where r is the radius at the axial station x, d is the maximum diameter of the AUV Hull and a is the AUV nose length Similarly, the shape of the tail is given as

$$\begin{aligned} r = \frac{d}{2} - \left\{\frac{3d}{2(100-a-b)^2} - \frac{\tan\alpha}{(100-a-b)}\right\}\{x-a-b\}^2 + \\ \left\{\frac{d}{(100-a-b)^3} - \frac{\tan\alpha}{(100-a-b)^2}\right\}\{x-a-b\}^3 \end{aligned} \tag{5.2}$$

where

- b: Length of the mid-hull of the AUV
- α: Semi angle of the tail section
- n: nose index which defines the nose curvature
- $100-a-b$: length of the tail section

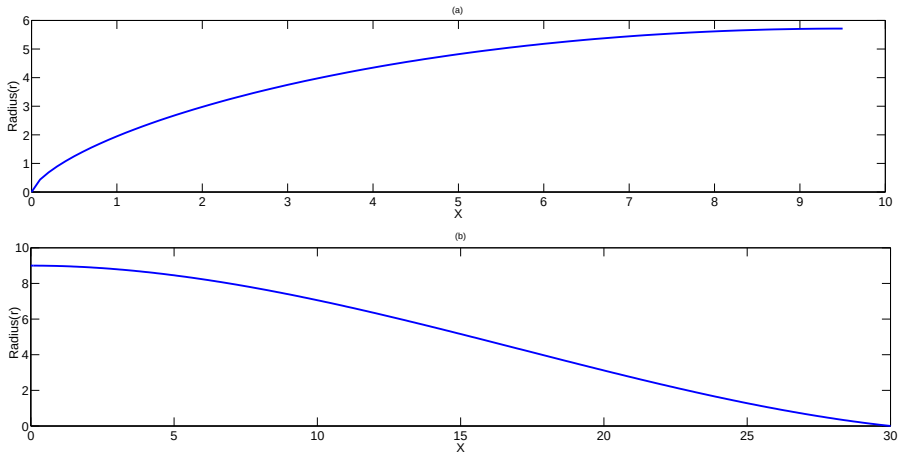

Figure 5.6: (a) Shape of the nose (b) Shape of the tail

The simulated models of these equations are shown in Fig.5.6. The CAD model of AUV is designed using Solidworks software and the following are the specification of the AUV structure. The nose and tail shapes are simulated in MATLAB using [49] formulation.

Thruster

The thruster used for robotic vehicles are brushed/brushless motor attached with a propeller which upon rotation pushes the AUV in the forward direction. The choice of thruster is chosen according to the AUV size and weight. The thruster Model-150 from Tecnadyne is suitable for our requirement as it has high efficiency. DC brushless motor provides 2.1 kg of forward thrust and 1.1kg of reverse thrust. The power supply required for this thruster is 12vdc, 24vdc or 48vdc and the speed and direction of rotation can be controlled using +/-5v analog input. It can be interfaced using RS232 or RS485 with any microcontroller or microprocessor. Following the weight of the thruster i.e. 0.7kg in air it can be found that this thruster is suitable for small or medium AUVs.

Control Planes

The designed AUV has four control planes utilized for navigation along the desired path. These control planes are designed using NACA 0012 wingspan dimensions for low drag. There are two rudder planes and two stern planes and these control planes are controlled with the help of four servo motors for rudder and stern planes.

5.5.2 Electrical Design

Navigation

- *Inertial Measurement Unit (IMU)*: IMUs are used for calculation of vehicle position and velocity. The IMU consists of a Gyrometer, an Acclerometer and a Magne-

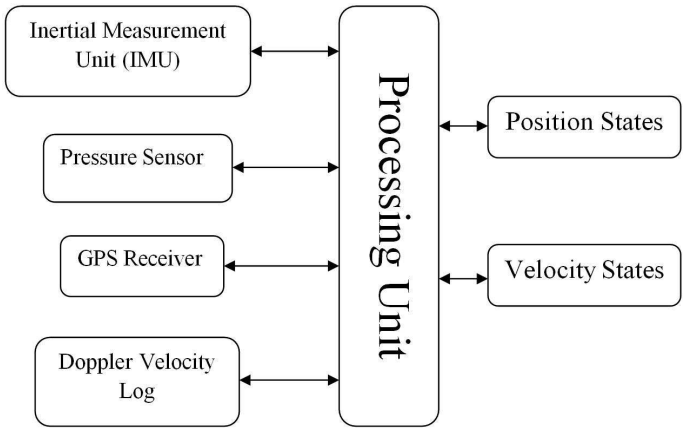

Figure 5.7: Multiple sensor fusion for the calculation of accurate AUV states

tometer, the raw data from the sensor are calibrated in an onboard microcontroller using Kalman filtering approach for estimation of position and velocity of AUV. The IMU which is utilized for the development of AUV setupin this work is Razor IMU from Sparkfun, it consists of triple-axis accelerometer (ADXL-345), triple-axis gyro (ITG-3200), triple-axis magnetometer (HMC5883L) and the onboard microcontroller (ATMega328). It can be directly programmed using Arduino software development package. Some of the other options for IMU are: CHR-UM6 from Pololu Robotics, MTI-Xsens,

- *Pressure Sensor*: To measure the depth of the AUV from the surface, a pressure sensor is to be interfaced. The maximum allowable depth with reference to surface is taken as 10m for which corresponding 30psi sensor is suitable. Taking these into consideration, the LM-31 from Measurement specialties is considered, this is a miniature pressure sensor capable of 30psi and corresponding output voltage is 0.5 to 4.5v. The supply voltage to this sensor is 5V DC supply.

- *GPS Receiver*: For underwater application, GPS might not work properly because of the weak satellite signal strength. Instead, it can be used while AUV is near to the surface. 66 Channel LS20031GPS from Sparkfun is chosen for implementation, it tracks up to 66 satellites with 10Hz of update rate.

- *Doppler Velocity Log (DVL)*: DVL sensors work in the principle of Doppler effect. It sends and receive sound signal reflected from the sea floor from which the velocity vector of the AUV is calculated. This information in combination of IMU results in accurate position and velocity of the AUV. The DVL of NavQuest has the smallest DVL, it is of 12.6cm diameter and 17cm in length. The maximum allowable depth is 110m and minimum is 0.3m with 1% accuracy. Due to its compact size and less weight this DVL is appropriate for small or midsized AUVs or ROVs.

Guidance

- *Sonar*: These sensors are used for avoiding the obstacles in the path and also for defense application these sensors can be used for mine countermeasure. An AUV consists of the following sensors i.e. forward-looking, down-ward looking and sidescan sonar. The images available from these sensors can be processed for identifying the specific objects. The sonar sensors which are available are not small enough to be used for small AUVs or ROVs but sensors from Imagenex Pvt.Ltd are significantly small and low weight. The sonar sensor can be implemented for different applications such as forward looking sonar, downward looking sonar and side-scan sonar.

- *USBL Tracking System*: Ultra Short Baseline(USBL) is a method for determining the location of AUV. A USBL system consists of transceiver and transponder, the transciever is attached with the mother ship or other surface vehicle and transponder is attached with the AUV or is placed at the sea floor. The transmitting and receiving of acoustic pulse between transciever and transponder are exchanged and this enables the USBL system to estimate the position of mother ship or the position of AUV with respect to mother ship. The USBL system which will be used for our AUV is MicroNav-USBL Tracking System from Tritech. This USBL system has the tracking range of $500m$ with the operating frequency of 20kHz to 28kHz.

Communication

- *Acoustic Modem*: Underwater communication is a method of exchanging data between the surface vehicle and underwater vehicle. Underwater communication encounters numerous difficulties such as multi-path propagation, small bandwidth and signal attenuation for long range communication. Keeping in view the above constraints the required modem for underwater communication should have low data rate. Taking these into consideration, the acoustic modem from Tritech Ltd is chosen for the AUV setup. Its data rate is approximately 40bps and the operating frequency is 20kHz to 24kHz with input power consumption is 8W maximum. The operating range is 500m horizontal and 150m vertical and input power supply is 12-24V. The USBL Tracking system will be interfaced with modem to acquire the vehicles actual velocities and send it to the surface unit.

Power Supply

- *DC-DC Convertor*: For a medium sized AUV which is equipped with DVL, acoustic modem, thruster etc, the overall power requirement is approximately within 200 to 400watt. The total power required for the AUV is 300watts, so the selected DC-DC

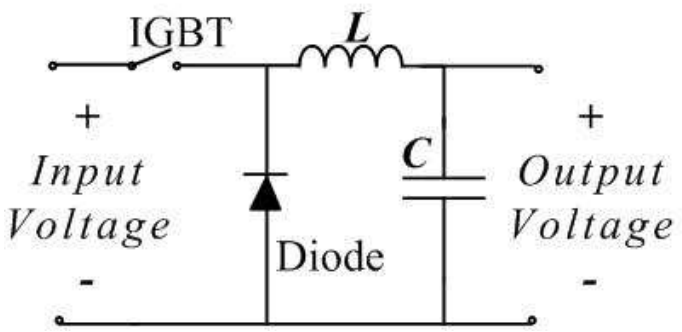

Figure 5.8: Circuit Diagram of DC-DC Convertor

convertor is JNC350R from Lineage Power of 350watt. The following DC-DC with typical 24v as the input voltage. The output of the convertor is 28v and maximum current it can provide is 12.5A. Fig.5.8 shows a circuit for DC-DC convertor, which provides step down output voltage. Also various power regulators can be utilized to derive particular voltages from 28v such as 3.3v, 5v and 12v as per the requirement by various subsystems.

- *Battery Bank*: Among various battery types like NiCd, NiMH,Lead Acid the Li-Po batteries are most suitable because it has higher gravimetric energy density which is nearly $100-130Wh/kg$. As compared to other batteries, the power carrying capacity per 1kg is more, which enables us to have same voltage at lighter weight. Due to these advantages it is mostly used for Underwater Vehicles.

Processing Unit

- *Single Board Computer(SBC)*: SBC is required for processing the data received from various sensors and to implement the control algorithm. The SBC can be considered as the brain of the AUV and takes necessary action for navigating the AUV towards the desired path. For this work, the roboard-110 SBC is chosen due to its wide range of input and output ports and for various functionality as mentioned in Table.5.1. The Roboard-110 is compatible with DOS, Windows 98/ME, Windows XP,Windows Embedded CE 6.0,Windows XP Embedded, Windows Embedded Standard, Linux distribution kernel 2.4.x, 2.6.x and it can also be programmed using Microsoft Robotic Studio. Due to its numerous functionalities and compatibility with many OS it is chosen as main SBC for AUV. Or also DSP controller [50] can be used for implementation of control algorithms.

- *Microcontroller*: Along with SBC, another processing unit is chosen for the interfacing of sensors and actuators based on Arduino platform. This platform uses ATmega2560 microcontroller with 54 digital I/O out of which 14 can be used as PWM

Processor	$DMPVortex86DX$
BIOS	AMI BIOS
Memory	256MB DDR2
ADCs	Analog Devices AD-7918 10-bit
I/O Interface	Micro SD slot x1, USB port x 1 (USB 2.0 version)
Power Consumption	+5V @ 400mA
Power Input	DC 6V to 24V
Outputs	PWM, Serial(COM 1, 2, 3,and 4), Hi-Speed Serial(COM 5 and COM 6), I2C
Compatible O/S	DOS, Windows 98/ME/XP, Windows Embedded CE, Linux
Dimension and Weight	96 x 56 mm, 40g

Table 5.1: Specifications of Single Board Computer(Roboard)

control, 4 serial ports and 16 analog inputs. These microcontrollers can be programmed through Windows based Arduino platform and can be easily downloaded into the microcontroller board.

5.6 Chapter Summary

In this chapter, a graphical visualization tool has been developed for analyzing the motion of single and multiple AUVs in graphical environment. The proposal for the hardware developed is also described for medium size AUV and also this chapter discusses about various sensors and actuators which can be interfaced to the AUV for necessary real-time control implementation.

Chapter 6

Conclusion and Scope of Future Work

6.1 Overall Summary of the thesis

This thesis addressed the path following control problem of an Autonomous Underwater Vehicle and also the formation control of multiple Autonomous Underwater Vehicles. As discussed in the objectives, the controllers for both path following problem and cooperative motion control problem have been developed.

The development of path following controller for an AUV has been successfully implemented using MATLAB & SIMULINK considering the nonlinearities and coupling terms in the dynamic equation. Lyapunov theory and backstepping concept have been used to develop path following controller for an AUV where the coupling of rudder angle between sway motion and yaw motion has been considered. Also the control of forward motion i.e. surge motion is included for forward motion control. The gains of the controller are also adapted according to the error derived while following the path.

The development of a formation control algorithm for multiple AUVs has been presented in Chapter 4. For the leader-follower formation strategy, it is required that the follower should follow the leader while maintaining a safe distance and orientation from the leader. It is assumed that only leader has the information of desired path and also the dynamics of leader and followers are perfectly matched. The controller for leader-follower method has been derived using backstepping method and it is also shown that the states of the AUV system remains bounded using the proposed backstepping control.

A graphical visualization has been also developed and it is discussed in Chapter 5. Due to multiple parameters such as hydrodynamic force, added mass, lift and drag force it is difficult to visualize the motion of AUV. Hence, a graphical simulation has been developed using Virtual Reality Modeling Language(VRML). After having studied the dynamics of AUV developed for both the path following and formation controller, the graphical simulation helps for designing a real hardware set-up for a single AUV. Subsequently for

developing AUV hardware, mechanical structure, AUV sensors and actuators have been selected.

6.1.1 Contributions of the Thesis

- This thesis has proposed a path following control algorithm using S-F frame and error backstepping approach for a single AUV considering the coupling of the rudder orientation in surge and sway equation of motion.
- Developed two leader-follower formation control algorithm for a group of AUVs using error backstepping approach and fuzzy logic technique.
- A graphical simulation platform is developed to visualize the effectiveness of the control strategies for both path following and formation control of AUV(s).
- Design of AUV body together with sensors and actuators for hardware setup has been proposed to build AUV control setup with necessary data acquisition systems.

6.2 Suggestions for the future work

In the thesis only 3DoF is considered in the dynamic equations and these are used for implementation of different controllers. However, the path following control development of a single AUV can be further extended by considering the complete 6DoF dynamic equations of motion.

The effects of ocean current has not been considered in the development of control law of the AUV. Hence, for real-world situation one has to certainly consider the above effect in the control development. Further, to address the uncertainties in the AUV parameters such as hydrodynamic effect and oceanic current a robust controller can be developed.

The formation control strategy described in Chapter 4 can be further extended as follows i.e. instead of assuming all the state parameters of leader AUV available, observers can be designed to estimate the unavailable/unmeasured states to cope up the real-world problems. The states of the leader AUV can be estimated by the follower AUVs and this can be used in the formation control.

The design of the hardware presented in Chapter 5 can be followed to realize the hardware AUV setup and subsequently for implementation of the developed path following controller.

Bibliography

[1] J. Ghommam, F. Mnif, A. Benali, and N. Derbel, "Nonsingular serret-frenet based path following control for an underactuated surface vessel," *Journal of Dynamic Systems, Measurement, and Control*, vol. 131, no. 2, p. 021006, 2009.

[2] K. Do, Z. Jiang, and J. Pan, "Robust adaptive path following of underactuated ships," *Automatica*, vol. 40, no. 6, pp. 929–944, 2004.

[3] C. Silvestre, "Multi-objective optimization theory with application to the integrated design of controllers/plants for autonomous vehicle," Ph.D. dissertation, Robot. Dept., Instituto Superior Technico (IST), Lisbon, Portugal, Jun. 2000.

[4] R. Wernli, "Auv commercialization-who's leading the pack?" in *OCEANS 2000 MTS/IEEE Conference and Exhibition*, vol. 1, Providence, RI, 2000, pp. 391–395.

[5] R. L. Wernli, "Auvs-a technology whose time has come," in *International Symposium on Underwater Technology*, Tokyo, Japan, 2002, pp. 309–314.

[6] P. E. Hagen, N. Storkersen, K. Vestgard, and P. Kartvedt, "The hugin 1000 autonomous underwater vehicle for military applications," in *OCEANS 2003. Proceedings*, vol. 2, San Diego, CA, USA, 2003, pp. 1141–1145.

[7] R. Panish, "Dynamic control capabilities and developments of the bluefin robotics auv fleet," in *Proc.* 16^{th} *Int. Symp. Unmanned Untethered Submersible Technology*, Durham, NH, USA, 2009.

[8] S. K. Das, D. Pal, S. Nandy, V. Kumar, S. N. Shome, and B. Mahanti, *Trends in Intelligent Robotics*. Springer, 2010, vol. 103, ch. Control Architecture for AUV-150: A Systems Approach, pp. 41–48.

[9] T. Copros and D. Scourzic, *Global Change: Mankind-Marine Environment Interactions*. Springer, 2011, ch. Alister-Rapid Environment Assessment AUV (Autonomous Underwater Vehicle), pp. 233–238.

[10] P. Maurya, E. Desa, A. Pascoal, E. Barros, G. Navelkar, R. Madhan, A. Mascarenhas, S. Prabhudesai, S. Afzulpurkar, A. Gouveia *et al.*, "Control of the maya auv in the vertical and horizontal planes: theory and practical results," in *Proceedings of the* 7^{th} *IFAC Conference on Manoeuvring and Control of Marine Craft*, Lisbon, Portugal, 2006.

[11] J. Kalwa, "The racun-project: Robust acoustic communications in underwater networks-an overview," in *OCEANS, 2011 IEEE-Spain*, Santander, Spain, 2011, pp. 1–6.

[12] H. Takahashi, H. Nishi, and K. Ohnishi, "Autonomous decentralized control for formation of multiple mobile robots considering ability of robot," *IEEE Transactions on Industrial Electronics*, vol. 51, no. 6, pp. 1272–1279, 2004.

[13] J. Guo, Z. Lin, M. Cao, and G. Yan, "Adaptive control schemes for mobile robot formations with triangularised structures," *IET Control Theory Applications*, vol. 4, no. 9, pp. 1817–1827, 2010.

[14] R. Beard, J. Lawton, and F. Hadaegh, "A coordination architecture for spacecraft formation control," *IEEE Transactions on Control Systems Technology,*, vol. 9, no. 6, pp. 777 –790, 2001.

[15] X. Wang, V. Yadav, and S. Balakrishnan, "Cooperative uav formation flying with obstacle/collision avoidance," *IEEE Transactions on Control Systems Technology*, vol. 15, no. 4, pp. 672–679, 2007.

[16] F. Borrelli, T. Keviczky, and G. Balas, "Collision-free uav formation flight using decentralized optimization and invariant sets," in *IEEE Conference on Decision and Control*, vol. 1, Nassau, Bahamas, 2004, pp. 1099–1104.

[17] T. Balch and R. C. Arkin, "Behavior-based formation control for multirobot teams," *IEEE Transactions on Robotics and Automation*, vol. 14, no. 6, pp. 926–939, 1998.

[18] R. Kumar and J. A. Stover, "A behavior-based intelligent control architecture with application to coordination of ¡ultiple underwater vehicles," *IEEE Transactions on Systems, Man and Cybernetics*, vol. 30, no. 6, pp. 767–784, 2000.

[19] J. R. T. Lawton, R. W. Beard, and B. J. Young, "A decentralized approach to formation maneuvers," *IEEE Transactions on Robotics and Automation*, vol. 19, no. 6, pp. 933–941, 2003.

[20] M. J. Mataric, "Behaviour-based control: examples from navigation, learning, and group behaviour," *Journal of Experimental and Theoretical Artificial Inteligence*, vol. 9, no. 2-3, pp. 323–336, 1997.

[21] M. A. Lewis and K. H. Tan, "High precision formation control of mobile robots using virtual structures," *Autonomous Robots*, vol. 4, no. 4, pp. 387–403, 1997.

[22] W. Ren and R. Beard, "A decentralized scheme for spacecraft formation flying via the virtual structure approach," *American Control Conference*, vol. 2, pp. 1746–1751, 2003.

[23] K. D. Do, "Formation tracking control of unicycle-type mobile robots with limited sensing ranges," *IEEE Transactions on Control Systems Technology*, vol. 16, no. 3, pp. 527–538, 2008.

[24] D. Sun, C. Wang, W. Shang, and G. Feng, "A synchronization approach to trajectory tracking of multiple mobile robots while maintaining time-varying formations," *IEEE Transactions on Robotics*, vol. 25, no. 5, pp. 1074–1086, 2009.

[25] J. Ghommam and F. Mnif, "Coordinated path-following control for a group of underactuated surface vessels," *IEEE Transactions on Industrial Electronics*, vol. 56, no. 10, pp. 3951–3963, 2009.

[26] J. Petrich and D. Stilwell, "Model simplification for auv pitch-axis control design," *Ocean Engineering*, vol. 37, no. 7, pp. 638–651, 2010.

[27] X. qin Cheng, Z. ping Yan, X. qian Bian, and J. jia Zhou, "Application of linearization via state feedback to heading control for autonomous underwater vehicle," in *IEEE International Conference on Mechatronics and Automation*, 2008, pp. 477–482.

[28] H. Khalil and J. Grizzle, *Nonlinear systems*. Macmillan Publishing Company, New York, 1992.

[29] M. Krstic, I. Kanellakopoulos, and P. Kokotovic, *Nonlinear and adaptive control design*, 1995.

[30] S. Patnaik, L. Jain, S. Tzafestas, G. Resconi, and A. Konar, *Innovations in Robot Mobility and Control*. Springer, 2006.

[31] J. Guo, F.-C. Chiu, and C.-C. Huang, "Design of a sliding mode fuzzy controller for the guidance and control of an autonomous underwater vehicle," *Ocean Engineering*, vol. 30, no. 16, pp. 2137–2155, 2003.

[32] J. Cheng, Y.Li, and D. Zhao, "Design of a sliding mode controller for trajectory tracking problem of marine vessels," *IET Control Theory Application*, vol. 1, no. 1, pp. 233–237, 2007.

[33] A. K. Deb and A. Juyal, "Adaptive neuro-fuzzy control of dynamical systems," in *International Joint Conference on Neural Networks (IJCNN)*, San Jose, CA, USA, 2011, pp. 2710–2716.

[34] Z.-P. Jiang and H. Nijmeijer, "Tracking control of mobile robots: A case study in backstepping," *Automatica*, vol. 33, no. 7, pp. 1393–1397, 1997.

[35] L. Lapierre and D. Soetanto, "Nonlinear path-following control of an auv," *Ocean Engineering*, vol. 34, no. 11-12, pp. 1734–1744, 2007.

[36] L. Lapierre and B. Jouvencel, "Robust nonlinear path-following control of an auv," *IEEE Journal of Oceanic Engineering*, vol. 33, no. 2, pp. 89–102, 2008.

[37] J. P. Desai, J. Ostrowski, and V. Kumar, "Controlling formations of multiple mobile robots," *IEEE Conference on Robotics and Automation*, vol. 4, pp. 2864–2869, 1998.

[38] J. Shao, G. Xie, and L. Wang, "Leader-following formation control of multiple mobile vehicles," *IET Control Theory Applications*, vol. 1, no. 2, pp. 545–552, 2007.

[39] L. Consolini, F. Morbidi, D. Prattichizzo, and M. Tosques, "Leader-follower formation control of nonholonomic mobile robots with input constraints," *Automatica*, vol. 55, no. 11, pp. 3944–3953, 2008.

[40] R. Cui, S. S. Ge, B. V. E. How, and Y. S. Choo, "Leader-follower formation control of underactuated autonomous underwater vehicles," *Ocean Engineering*, vol. 37, no. 17, pp. 1491–1502, 2010.

[41] K. Choi, S. J. Yoo, J. B. Park, and Y. H. Choi, "Adaptive formation control in absence of leader's velocity information," *IET Control Theory Applications*, vol. 4, no. 4, pp. 521–528, 2010.

[42] M. Sisto and D. Gu, "A fuzzy leader-follower approach to formation control of multiple mobile robots," in *IEEE/RSJ International Conference on Intelligent Robots and Systems*, Beijing, 2006, pp. 2515–2520.

[43] M. Defoort, T. Floquet, A. Kksy, and W. Perruquetti, "Sliding-mode formation control for cooperative autonomous mobile robots," *IEEE Transactions on Industrial Electronics*, vol. 55, no. 11, pp. 3944–3953, 2008.

[44] P. Ogren, M. Egerstedt, and X. Hu, "A control lyapunov function approach to multiagent coordination," *IEEE Transactions on Robotics and Automation*, vol. 18, no. 5, pp. 847–851, 2002.

[45] H. Mehrjerdi, J. Ghommamb, and M. Saad, "Nonlinear coordination control for a group of mobile robots using a virtual structure," *Mechatronics*, vol. 21, no. 7, pp. 1147–1155, 2011.

[46] G. Antonelli, F. Arrichiello, and S. Chiaverini, "Experiments of formation control with collisions avoidance using the null-space-based behavioral control," in 14^{th} *Mediterranean Conference on Control and Automation*, Ancona, Italy, 2006, pp. 1–6.

[47] L. Lapierre, D. Soetanto, and A. Pascoal, "Nonlinear path following with applications to the control of autonomous underwater vehicles," in *IEEE conference on Decision and Control*, ser. 16, vol. 2, Maui, HI, 2003, pp. 1256–1261.

[48] S. Banerjee, T. Kumar, J. Pal, and D. Prasad, "Controller design for large-gap control of electromagnetically levitated system by using an optimization technique," *IEEE Transactions on Control Systems Technology*, vol. 16, no. 3, pp. 408–415, 2008.

[49] D. F. Myring, "A theoretical study of body drag in sub-critical axisymmetric flow," *Aeronautical Quaterly*, vol. 27, no. 3, pp. 186–194, 1976.

[50] S. A. Hariprasad and R. Nagaraj, "An efficient method of controlling ac power using dsp 2407-a controller," *International Journal of Computer Science and Network Security (IJCSNS)*, vol. 8, no. 9, p. 297, 2008.

[51] T. Fossen, *Guidance and Control of Ocean Vehicles*. New York: Wiley, 1994, ch. 2, pp. 6–55.

Appendices

Appendix A

Kinematics and Dynamics of an AUV

A.1 Kinematics

The kinematics equations of AUV or other autonomous vehicle are generally represented using two coordinate frames i.e. earth-fixed frame and body-fixed frame [51]. The velocity parameters of the AUV are determined from the body-fixed frame and using a transformation matrix, the velocity in the earth-fixed frame is determined. Referring Table A.1 where the AUV parameters are categorized as Earth-Fixed frame(E-F) and Body-Fixed frame(B-F).

The transformation matrix $J_1(\eta)$ and $J_2(\eta)$ are defined as follows,

$$J_1(\eta_2) = \begin{bmatrix} Cos(\psi) & -Sin(\psi) & 0 \\ Sin(\psi) & Cos(\psi) & 0 \\ 0 & 0 & 1 \end{bmatrix} \begin{bmatrix} Cos(\theta) & 0 & Sin(\theta) \\ 0 & 1 & 0 \\ -Sin(\theta) & 0 & Cos(\theta) \end{bmatrix} \begin{bmatrix} 1 & 0 & 0 \\ 0 & Cos(\phi) & -Sin(\phi) \\ 0 & Sin(\phi) & Cos(\phi) \end{bmatrix} \tag{A.1}$$

$$J_2(\eta_2) = \begin{bmatrix} 1 & Sin(\phi)Tan(\theta) & Cos(\phi)Tan(\theta) \\ 0 & Cos(\phi) & -Sin(\phi) \\ 0 & Sin(\phi)/Cos(\theta) & Cos(\phi)/Cos(\theta) \end{bmatrix} \tag{A.2}$$

where, $J_1(\eta_2)$ is utilized for the conversion of body-fixed linear velocities(u, v, w) to earth-fixed linear velocities$(\dot{x}, \dot{y}, \dot{z})$ and $J_2(\eta_2)$ is used for converting the body-fixed angular velocities(p, q, r) to earth-fixed angular velocities$(\dot{\phi}, \dot{\theta}, \dot{\psi})$.

Table A.1: Position and velocities of the AUV

Motion Direction	E-F Frame(position)	B-F Frame(velocity)
Surge	x	u
Sway	y	v
Heave	z	w
Roll	ϕ	p
Pitch	θ	q
Yaw	ψ	r

The complete transformation between body-fixed and earth-fixed frames represent the kinematics equation of the AUV which is given as follows,

$$\begin{bmatrix}\dot{\eta}_1\\ \dot{\eta}_2\end{bmatrix} = \begin{bmatrix}J_1(\eta_2) & 0_{3\times3}\\ 0_{3\times3} & J_2(\eta_2)\end{bmatrix}\begin{bmatrix}\nu_1\\ \nu_2\end{bmatrix} \tag{A.3}$$

where, $\dot{\eta}_1 = [\dot{x}, \dot{y}, \dot{z}]^T$ and $\dot{\eta}_2 = \left[\dot{\phi}, \dot{\theta}, \dot{\psi}\right]^T$ represents the AUV velocities in the earth-fixed frame. The corresponding body-fixed velocities of the AUV are $\nu_1 = [u, v, w]$ and $\nu_2 = [p, q, r]$.

A.2 Dynamics

Dynamics of the AUV consists of nonlinearity and coupling between various terms. The AUV has 6DOF equation of motion along x,y and z axis, the following are the dynamic equation along the respective axis.

- Surge Motion:

$$m\left[\dot{u} - vr + wq - x_g(q^2 + r^2) + y_g(pq - \dot{r}) + z_g(pr + \dot{q})\right] = X \tag{A.4}$$

- Sway Motion

$$m\left[\dot{v} - wp + ur - y_g(p^2 + r^2) + z_g(qr - \dot{p}) + x_g(pq + \dot{r})\right] = Y \tag{A.5}$$

- Heave Motion

$$m\left[\dot{w} - uq + vp - z_g(q^2 + p^2) + x_g(pr - \dot{q}) + y_g(qr + \dot{p})\right] = Z \tag{A.6}$$

- Roll Motion

$$\begin{aligned} I_x\dot{p} + (I_z - I_y)qr - (\dot{r} + pq)I_{xz} + (r^2 - q^2)I_{yz} + (pr - \dot{q})I_{xy} + \\ m\left[y_g(\dot{w} - uq + vp) - z_g(\dot{v} - wp + ur)\right] = K \end{aligned} \tag{A.7}$$

- Pitch Motion

$$\begin{aligned} I_y\dot{q} + (I_x - I_z)pr - (\dot{p} + qr)I_{xy} + (p^2 - r^2)I_{zx} + (qp - \dot{r})I_{yz} + \\ m\left[z_g(\dot{u} - vr + wq) - x_g(\dot{w} - uq + vp)\right] = M \end{aligned} \tag{A.8}$$

- Yaw Motion

$$\begin{aligned} I_z\dot{r} + (I_y - I_x)pq - (\dot{q} + rp)I_{yz} + (q^2 - p^2)I_{xy} + (rq - \dot{p})I_{zx} + \\ m\left[x_g(\dot{v} - wp + ur) - y_g(\dot{u} - vr + wq)\right] = N \end{aligned} \tag{A.9}$$

Table A.2: AUV parameter definition

Hydrostatic Force	$X_{HS}, Y_{HS}, Z_{HS}, K_{HS}, M_{HS}, N_{HS}$
Added Mass	$X_{\dot{u}}, Y_{\dot{v}}, Z_{\dot{w}}, K_{\dot{p}}, M_{\dot{w}}, Y_{\dot{r}}, Z_{\dot{q}}, M_{\dot{q}}, N_{\dot{v}}, N_{\dot{r}}$
Propeller Thrust	X_{prop}
Lift Force	$Z_{uu\delta_s}, Y_{uu\delta_r}, N_{uu\delta_r}$
Drag Force	$M_{ww}, M_{qq}, X_{uu}, Y_{vv}$

The parameterX, Y, Z, K, M, N are the external forces and moments, which includes Hydrostatic force, drag force, Lift force, Propeller Thrust, Added Mass and also the effect of stern plane and rudder planes. These external parameters are defined as follows,

$$\begin{aligned}
X =& X_{HS} + X_{u|u|}u\,|u| + X_{\dot{u}}\dot{u} + X_{wq}wq + X_{qq}qq + X_{vr}vr + X_{rr}rr + X_{prop} \\
Y =& Y_{HS} + Y_{v|v|}v\,|v| + Y_{r|r|}r\,|r| + Y_{\dot{v}}\dot{v} + Y_{\dot{r}}\dot{r} + Y_{ur}ur + Y_{wp}wp + Y_{pq}pq + Y_{uv}uv + \\
& Y_{uu\delta_r}u^2\delta_r \\
Z =& Z_{HS} + Z_{w|w|}w\,|w| + Z_{q|q|}q\,|q| + Z_{\dot{w}}\dot{w} + Z_{\dot{q}}\dot{q} + Z_{uq}uq + Z_{vp}vp + Z_{rp}rp + Z_{uw}uw + \\
& Z_{uu\delta_s}u^2\delta_s \\
K =& K_{HS} + K_{p|p|}p\,|p| + K_{\dot{p}}\dot{p} + K_{prop} \\
M =& M_{HS} + M_{w|w|}w\,|w| + M_{q|q|}q\,|q| + M_{\dot{w}}\dot{w} + M_{\dot{q}}\dot{q} + M_{uq}uq + M_{vp}vp + M_{rp}rp + \\
& M_{uw}uw + M_{uu\delta_s}u^2\delta_s \\
N =& N_{HS} + N_{v|v|}v\,|v| + N_{r|r|}r\,|r| + N_{\dot{v}}\dot{v} + N_{\dot{r}}\dot{r} + N_{ur}ur + N_{wp}wp + N_{pq}pq + \\
& N_{uv}uv + N_{uu\delta_r}u^2\delta r
\end{aligned} \tag{A.10}$$

the parameter used in (A.10) are defined in table.A.2. These parameters are the external components which affect the overall dynamics of the Autonomous Underwater Vehicle.

Appendix B

Parameters of the AUV Considered for Control

The INFANTE AUV [3] parameters are considered for verifying the control algorithm.

Table B.1: AUV parameters

m	2234.5Kg	I_x	$700Nms^2$
B	21898N	I_y	$1700Nms^2$
ρ	$1030Kgm^-3$	I_z	$2000Nms^2$
CB	(0 0 -0.041)	I_{xy}	0
CG	(0 0 0)	I_{yz}	0
L	4.215	I_{xz}	0

Table B.2: INFANTE AUV Hydrodynamic coefficients

$C_{x_{\dot{u}}} = \frac{\rho}{2}L^3X_{\dot{u}}$	-141.9	$C_{X_{rr}} = \frac{\rho}{2}L^4X_{rr}$	832	$C_{y_{\dot{v}}} = \frac{\rho}{2}L^3Y_{\dot{v}}$	-1715.4
$C_{Y_{rr}} = \frac{\rho}{2}L^4Y_{rr}$	-32.5	$C_{y_{\dot{r}}} = \frac{\rho}{2}L^4Y_{\dot{r}}$	186.9	$C_{Y_{vv}} = \frac{\rho}{2}L^2Y_{vv}$	-667.5
$C_{z_{\dot{w}}} = \frac{\rho}{2}L^3Z_{\dot{w}}$	-4617	$C_{N_{vv}} = \frac{\rho}{2}L^3N_{vv}$	433.8	$C_{z_{\dot{q}}} = \frac{\rho}{2}L^4Z_{\dot{q}}$	-1701.9
$C_{N_{rr}} = \frac{\rho}{2}L^5N_{rr}$	-310	$C_{k_{\dot{q}}} = \frac{\rho}{2}L^4K_{\dot{q}}$	-40.6	$C_{X_{wq}} = \frac{\rho}{2}L^3X_{wq}$	137
$C_{M_{\dot{w}}} = \frac{\rho}{2}L^4M_{\dot{w}}$	-2090.4	$C_{X_{w\delta s}} = \frac{\rho}{2}L^2X_{w\delta s}$	-221.7	$C_{M_{\dot{q}}} = \frac{\rho}{2}L^5M_{\dot{q}}$	-1692.3
$C_{X_{\delta s\delta s}} = \frac{\rho}{2}L^2X_{\delta s\delta s}$	-455	$C_{N_{\dot{v}}} = \frac{\rho}{2}L^4N_{\dot{v}}$	957	$C_{X_{\delta r\delta r}} = \frac{\rho}{2}L^2X_{\delta r\delta r}$	-80.3
$C_{N_{\dot{r}}} = \frac{\rho}{2}L^5N_{\dot{r}}$	-1349	$C_{X_{q\delta s}} = \frac{\rho}{2}L^3X_{q\delta s}$	-308.9	$C_{X_{uu}} = \frac{\rho}{2}L^2X_{uu}$	-35.4
$C_{Y_{\delta r}} = \frac{\rho}{2}L^2X_{\delta r}$	117.2	$C_{X_{vv}} = \frac{\rho}{2}L^2X_{vv}$	-128	$C_{Z_{\delta s}} = \frac{\rho}{2}L^2Z_{\delta s}$	-689.7
$C_{X_{ww}} = \frac{\rho}{2}L^2X_{ww}$	-89.48	$C_{M_{\delta s}} = \frac{\rho}{2}L^3M_{\delta s}$	-791.3	$C_{X_{qq}} = \frac{\rho}{2}L^4X_{qq}$	9587.4
$C_{N_{\delta r}} = \frac{\rho}{2}L^3N_{\delta r}$	-266				

Publications From This Thesis

- R. Rout, B. Subudhi and S. Ghosh,"Adaptive Path Following Control of an Autonomous Underwater Vehicle", *Proc. Advances in Control and Optimization of Dynamical Systems (ACODS2012)*, Bangalore, 16-18 Feb. 2012.
- R. Rout, B. Subudhi and S. Ghosh,"Backstepping Approach for Formation Control of Multiple Autonomous Underwater Vehicles using Leader-Follower Strategy", *Robotics and Autonomous Systems, Elsevier* (Submitted in Jan. 2012.).

Author's Biography

Raja Rout was born to Sri. Ashok Kumar Rout and Smt. Promodini Rout on 3^{rd} June, 1987 at Kendrapara, Odisha, India. He obtained a Bachelors degree in Applied Electronics and Instrumentation Engineering from Biju Patanaik University of Technology (B.P.U.T), Rourkela, Odisha in 2008. He joined the Department of Electrical Engineering, National Institute of Technology, Rourkela in January 2010 as an Institute Research Scholar to pursue M.Tech by Research.